AD-A075 978 ARMY ELECTRONICS RESEARCH AND DEVELOPMENT COMMAND WS--ETC F/G 4/2
PRECIPITATION ESTIMATION USING SATELLITE DATA.(U)
SEP 79 B T MIERS

UNCLASSIFIED ERADCOM/ASL-TR-0039 NL

/ OF /
AD
A075978

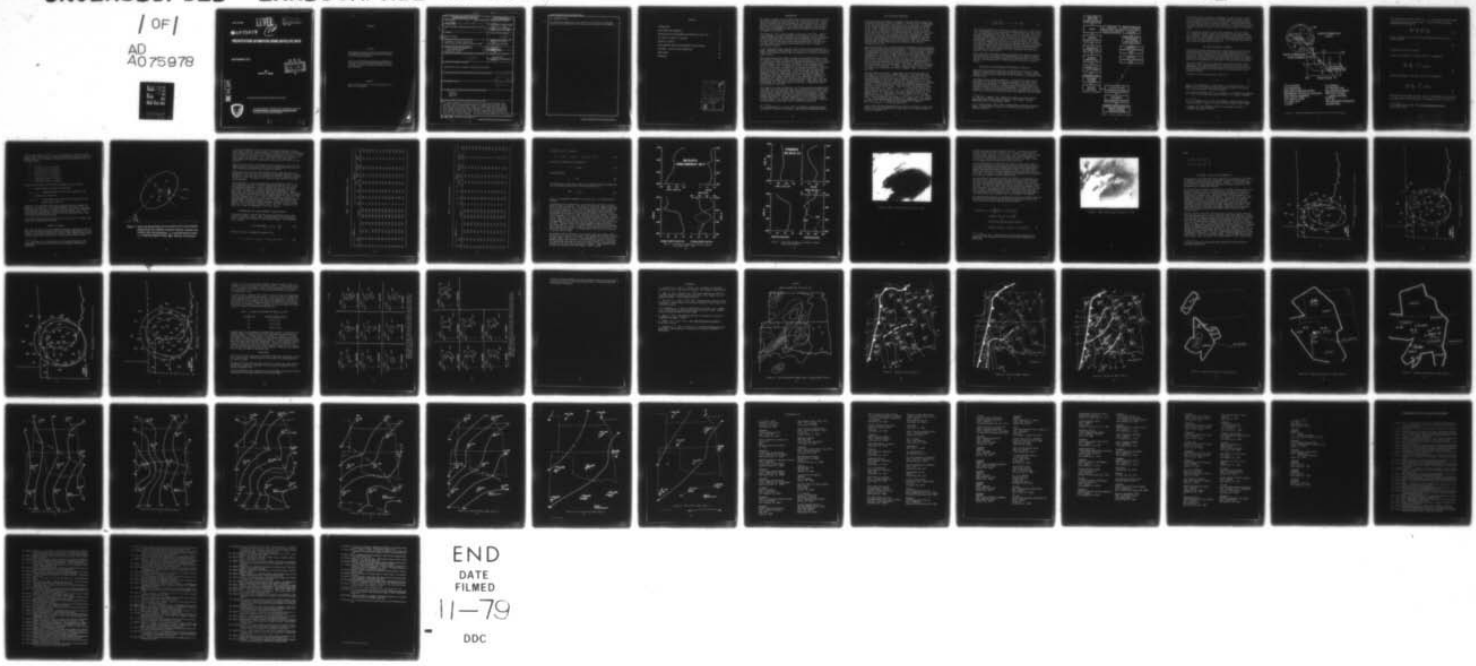

END
DATE
FILMED
11-79
DDC

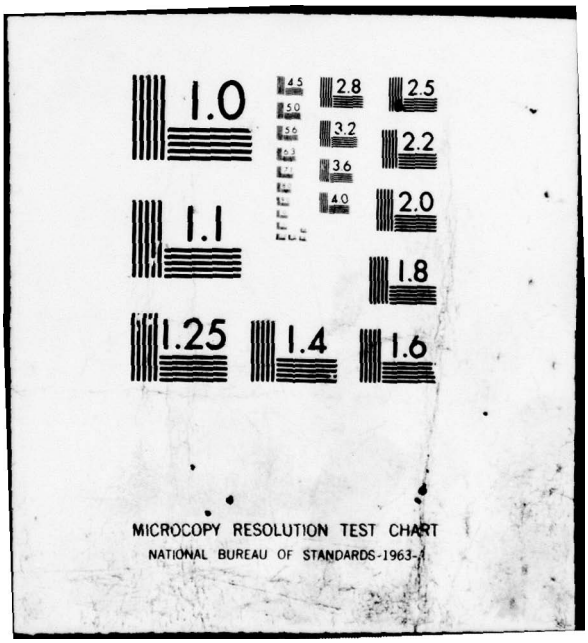
1.0
1.1
1.25
1.4
1.6
1.8
2.0
2.2
2.5
2.8
3.2
3.6
4.0
4.5
5.0
5.6
MICROCOPY RESOLUTION TEST CHART
NATIONAL BUREAU OF STANDARDS-1963-A

ASL-TR-0039

LEVEL II

AD

Reports Control Symbol
OSD 1366

AD A075978

PRECIPITATION ESTIMATION USING SATELLITE DATA

SEPTEMBER 1979

By
Bruce T. Miers

Approved for public release; distribution unlimited

US Army Electronics Research and Development Command
ATMOSPHERIC SCIENCES LABORATORY
White Sands Missile Range, NM 88002

NOTICES

Disclaimers

The findings in this report are not to be construed as an official Department of the Army position, unless so designated by other authorized documents.

The citation of trade names and names of manufacturers in this report is not to be construed as official Government indorsement or approval of commercial products or services referenced herein.

Disposition

Destory this report when it is no longer needed. Do not return it to the originator.

(14) ERADCOM/ASL-TR-0039

SECURITY CLASSIFICATION OF THIS PAGE (When Data Entered)

REPORT DOCUMENTATION PAGE

READ INSTRUCTIONS BEFORE COMPLETING FORM

1. REPORT NUMBER: ASL-TR-0039	2. GOVT ACCESSION NO.
3. RECIPIENT'S CATALOG NUMBER	
4. TITLE (and Subtitle): PRECIPITATION ESTIMATION USING SATELLITE DATA.	5. TYPE OF REPORT & PERIOD COVERED: R&D Technical Report.
	6. PERFORMING ORG. REPORT NUMBER
7. AUTHOR(s): Bruce T. Miers	8. CONTRACT OR GRANT NUMBER(s): (17) 21
9. PERFORMING ORGANIZATION NAME AND ADDRESS: Atmospheric Sciences Laboratory, White Sands Missile Range, New Mexico 88002	10. PROGRAM ELEMENT, PROJECT, TASK AREA & WORK UNIT NUMBERS: (16) DA Task 1L162111AH71-21
11. CONTROLLING OFFICE NAME AND ADDRESS: US Army Electronics Research and Development Command, Adelphi, MD 20783 (11)	12. REPORT DATE: September 1979 13. NUMBER OF PAGES: 46
14. MONITORING AGENCY NAME & ADDRESS (if different from Controlling Office): (12) 57	15. SECURITY CLASS. (of this report): UNCLASSIFIED 15a. DECLASSIFICATION/DOWNGRADING SCHEDULE

16. DISTRIBUTION STATEMENT (of this Report)

Approved for public release; distribution unlimited.

17. DISTRIBUTION STATEMENT (of the abstract entered in Block 20, if different from Report)

18. SUPPLEMENTARY NOTES

19. KEY WORDS (Continue on reverse side if necessary and identify by block number)

Rainfall
Satellite
Mesoscale

20. ABSTRACT (Continue on reverse side if necessary and identify by block number)

This report attempts to show that, by fitting particular nonlinear auto-covariance and cross-covariance functions to space-time covariance values calculated from satellite data, convective complex characteristics such as size, ellipticity, motion, growth, and decay of a storm can be determined. These modeled features then can be related to convective storm characteristics found by Scofield and Oliver. In turn, these characteristics are related to actual rainfall amounts. The results of this study are a first step CONT'

DD FORM 1 JAN 73 1473 EDITION OF 1 NOV 65 IS OBSOLETE

SECURITY CLASSIFICATION OF THIS PAGE (When Data Entered)

410 663

JCB

20. ABSTRACT (cont)

Cont'

in removing the subjectivity from current rainfall estimation techniques. Results from the 20 May 1977 storm over Texas and Oklahoma are presented.

CONTENTS

INTRODUCTION

The effects of weather on the planning for and execution of combat missions have been apparent to military men as long as man has fought man. Historically, the weather has been considered to a great extent to be a natural obstacle, akin to difficult terrain, about which soldiers could do little but accept the consequences. And unlike natural obstacles, the weather often varied considerably and was difficult to predict; one had to expect and prepare for the worst.

Trafficability is of critical concern to the army in the field. Battlefield commanders must have information on fluctuations in soil moisture content to make decisions concerning tactical maneuvers on the battlefield. Soil moisture conditions at a given time and place are a function of: (1) water input to the ground surface from precipitation, (2) water loss from the surface by evaporation and transpiration, and (3) changes in soil moisture storage.

In this study the primary concern is with item (1) of the preceding paragraph. Knowledge of where and when rain is occurring as well as the rate of rainfall will provide critical data on changes in soil moisture and thus on trafficability.

Much of the research work which is aimed at using satellite data to arrive at estimates of rainfall amounts has been very subjective in nature; that is, each person viewing the satellite imagery may interpret it in a slightly different manner, thus arriving at variations in the estimated surface rainfall amounts. The elimination of as much of this subjectivity as possible is desirable. An example of this subjective approach is Scofield and Oliver's[1] work which made use of infrared (IR) data to make quantitative estimates of cloud heights. Rainfall estimates were made from enhanced IR satellite images based on the premise that the higher the cumulonimbus cloud top the heavier the rain. Additional information on the rate of anvil growth, the position of the cumulonimbus under the spreading anvil, merging cells, merging convective cloud lines, and overshooting tops has been used to improve the model. These factors are then incorporated into a decision tree to aid the user in determining where and how much rain has fallen.

This study will attempt to show that, by fitting particular nonlinear autocovariance and cross-covariance functions to space-time covariance values calculated from satellite data, storm characteristics such as size, ellipticity, motion, growth, and decay of a storm can be determined. These modeled characteristics then can be related to storm features found by Scofield and Oliver.[1] The storm features in turn are related to actual rainfall amounts. The results of this study are a first step in removing the subjectivity from current rainfall estimation techniques.

---

[1]R. A. Scofield and V. J. Oliver, 1977, "A Scheme for Estimating Convective Rainfall from Satellite Imagery," NOAA Technical Memorandum NESS 86

DATA PROCESSING PROCEDURES

The Geostationary Operational Environmental Satellite (GOES) surveys the earth from a nominal altitude of 35,800 km. The GOES has a rotation speed of 100 rpm which generates a west-to-east scan of the earth. A stepping mirror allows the sensors to accomplish the north-to-south scan of the earth. Eight visible and two IR sensors, with resolutions of 1 by 1 km and 4 by 8 km, respectively, provide the data base. In one revolution of the satellite, the earth is scanned for about 18 degrees with each scan consisting of data from one IR sensor and eight visual sensors. These data are transmitted to the command station at a 28-megabit/s rate and then are time-stretched to fill the remaining 342 degrees of satellite rotation and retransmitted back to the satellite. GOES then retransmits the data back to earth where they are available to the users by a 2-megabit/s data rate.

When the satellite signal is received at the Atmospheric Sciences Laboratory (ASL) Direct Readout Ground Station (DRGS), it is processed through the Bit Frame Synchronizer/Sectionizer System (BFSSS). First the signal is detected and demodulated to digital baseband nonreturn to zero-level (NRZL) code by a demodulator. The signal is then routed to two bit synchronizers, one dedicated to infrared and the other to visible. The outputs of the bit synchronizers, each consisting of NRZL data and bit clock, are routed to the digital interface where the interface establishes synchronization on the IR signal and determines the transmission mode. Synchronization is then established on the visible signal. The digital interface is operated by a PDP 11/45 minicomputer. Through a computer program, sectors of data of interest to a researcher are stored on magnetic tape or displayed in real time.

Once the sector of interest is determined, the IR and visible data are separated into two files for further processing. Often when GOES data are viewed on a display monitor, it is obvious that entire lines of data are unacceptable for use in an analysis program, and random errors are sometimes present in the data. These errors require the use of a filtering and smoothing program to render the data acceptable for use in analysis programs. In outline form the filtering and smoothing program handles the data in the following manner. Image positions are defined by rectangular coordinates (i, j) where $i = 1, 2, \ldots, N$ gives the relative horizontal position (pixel) and $j = 1, 2, \ldots, M$ gives the relative position from the top of the image (line); and image intensity at point (i, j) is denoted by $F(i, j)$. Examination of the data showed that bad isolated points were characterized by $F(i, j) > \theta_1$, or $F(i, j) < \theta_2$. For visible data, θ_1 was assigned the value 59 and θ_2 the value 4; while for IR data, θ_1 and θ_2 were assigned values of 252 and 4, respectively. An isolated bad point, $F(i, j)$, is replaced by the average of its neighbors $F(i - 1, j)$ and $F(i + 1, j)$ on the same line j.

Unacceptable lines were characterized by rapid oscillations of intensities along a line and are detected by a large value of the "average slope" of the line by equation (1).

$$A = \frac{1}{N} \sum_{i=1}^{N-1} \left| F(i + 1, j) - F(i, j) \right|. \qquad (1)$$

The lines were defined as bad when A was greater than five. After examining a large number of cases, the author found that good lines have a value of A less than three and bad lines have a value of A near 20. In actual computer implementation, lines are processed first and random points next. The program also allows up to three consecutive bad lines or bad points before default of the entire data set. For the purposes of this study, the data were segmented so that only one convective complex will appear in a data set. Tests[2] have shown that the complete data set could possibly show some decimation while still producing the same covariance structure. The results of this study were derived by using every fifth pixel and every second line in the infrared and every twentieth pixel and every sixteenth line in the visible.

After this facet of the data processing procedure was complete, latitude and longitude for each point of the decimated data set were calculated. The data file and the latitude-longitude file were then used to calculate the raw covariance matrices. A data processing flow chart is shown in figure 1.

NAVIGATION FOR GEOSYNCHRONOUS METEOROLOGICAL SATELLITES

The navigation algorithm used by the ASL Meteorological Analysis System (AMAS) is a modification of Phillips and Smith's work.[3] Similar software packages are being used by NASA/GSFC and the Universities of Wisconsin and Colorado State.

The purpose of the navigation software is to provide the capability for accurately calculating the latitude and longitude of any point in the image data and, conversely, for computing the position on the image of any specified earth location. The data required to perform these transformations consist of four principal components: (1) spacecraft orbital elements for computing satellite position at any specified time, (2) spacecraft spin axis attitude, specified by the right ascension and declination

---

[2]A. Eddy and L. Hembree, 1977, "Space-Time Sampling from SMS Satellite Data Required to Define Convective Storms," Final Report, Contract DAAG29-76-D-0100, US Army Research Office

[3]D. R. Phillips and E. Smith, 1974, "Geosynchronous Satellite Navigation Model," Internal Report, University of Wisconsin Space Sciences and Engineering Center

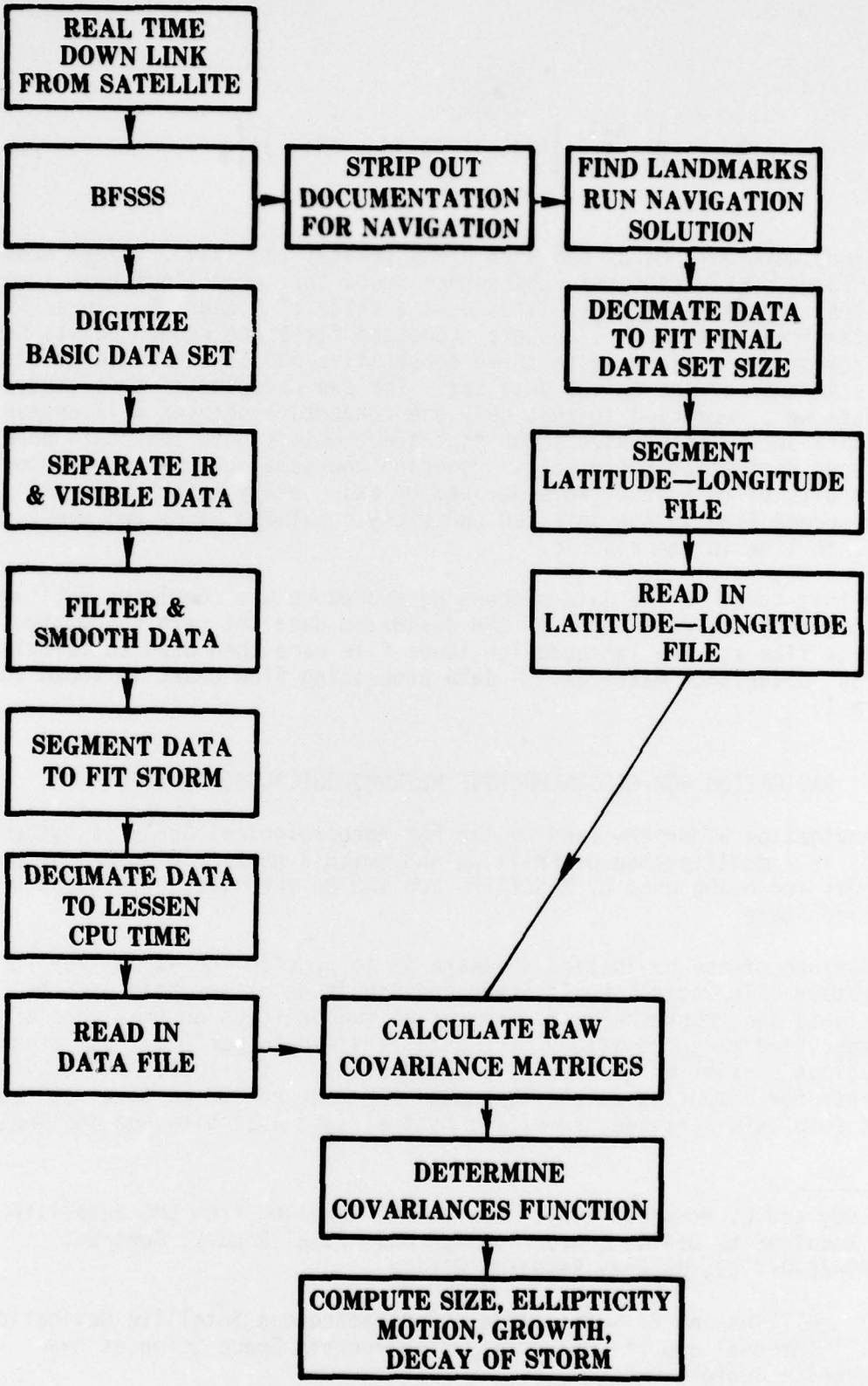

Figure 1. Data processing flowchart.

of the spin vector in celestial coordinates, (3) small angles of pitch, roll, and yaw that specify the misalignment between instrument optical axes and spacecraft spin axis and, (4) scan phase correction parameters for each image to which the navigation applies. These parameters (item (4) above) are the initial offset and drift rate, in the pixel (horizontal) direction, between the center of the earth and the center of the master image.

Three coordinate systems are used in the navigation solution, namely: (1) a celestial inertial system for description of orbit and attitude, (2) a geographic system rotating with the earth for description of landmarks, and (3) a time dependent satellite coordinate system for description of the scanning geometry (figure 2). For a detailed description of this solution, consult Billingsley et al.[4]

THE OBJECTIVE ANALYSIS TECHNIQUE

The objective analysis technique used in this project requires that the intrarelationships existing within each single parameter data set, as well as the interrelationships existing between these data sets, be determined. These relationships are then described in terms of correlation and cross-correlation functions which model the spatial and temporal structure of the phenomenon as reflected in the observations themselves.

The analysis model used is an extension[5] of classical multiple linear regression. This extension consists of modeling the structure that is representative of the information contained in the time series data set being analyzed and then using that model in the determination of the regression weights.

The model for the univariate case is given by

$$Y = X\beta + \varepsilon \,, \qquad (2)$$

where Y, the predictand, is an NX1 matrix; X, the predictor set, is an NXM matrix; β, the vector of regression weights, forms an MX1 matrix; and ε, the noise vector, forms an NX1 matrix.

In classical regression, If $E[\varepsilon] = 0$, where E is the expectation operator, $V\sigma^2 = E[\varepsilon\varepsilon^t]$ is the variance-covariance matrix of ε, where ε^t denotes

---

[4]J. J. Billingsley et al., 1977, "AOIPS METPAK, A Meteorological Data Processing System," Computer Science Corporation Report CSC/SD-77/6084

[5]A. Eddy, 1973, "The Objective Analysis of Atmospheric Structure," J Meteorol Soc Japan, 51:450-57

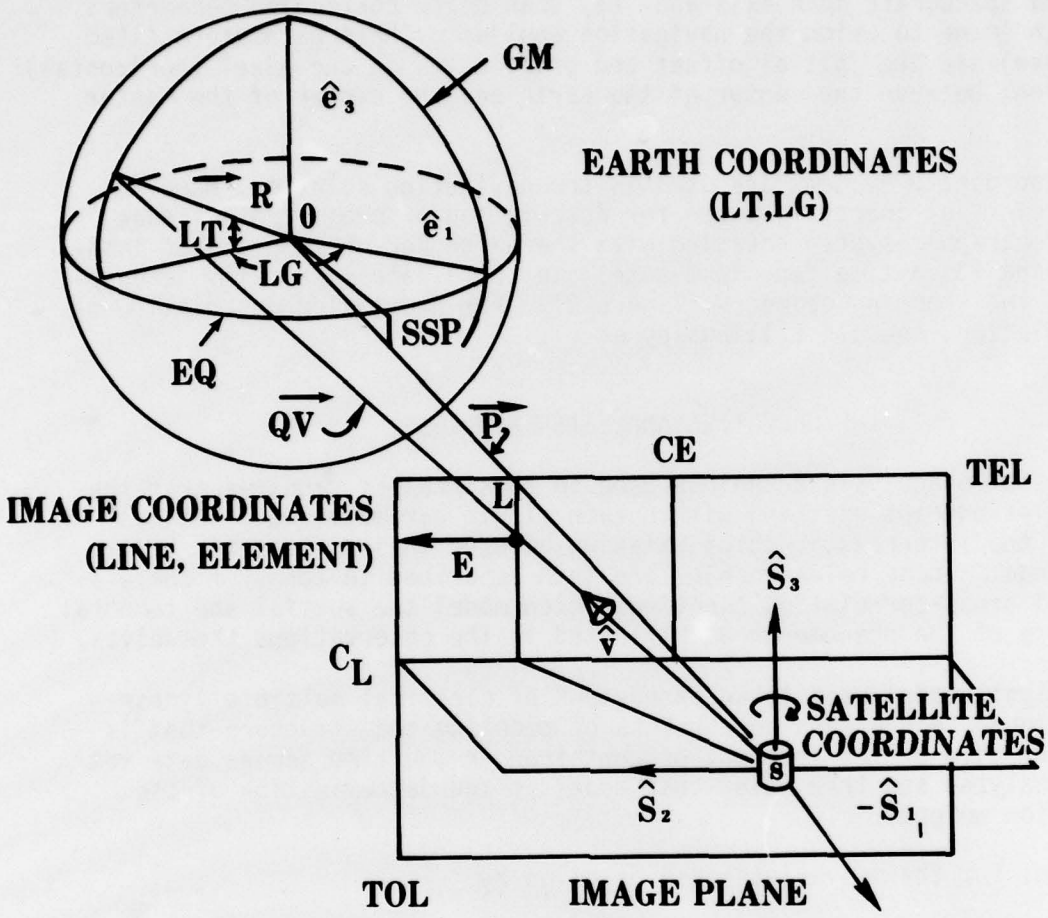

LT=LATITUDE
LG=LONGITUDE
SSP=SUB SATELLITE POINTS
$\overline{P}$=POSITION VECTOR OF SATELLITE
TEL=TOTAL ELEMENTS
TOL=TOTAL LINES
$\hat{S}$ = SPIN AXIS
L=LINE

E=ELEMENT
CL=CENTER LINE
CE=CENTER ELEMENT
$\overline{QV}$=VIEW VECTOR
$\underline{e}$=BASIS VECTORS
$\overline{R}$=$\overline{P}$- $\overline{QV}$
GM=GREENWICH MERIDIAN
EQ=EQUATOR

Figure 2. Relation between satellite, earth, and image coordinates.

the transpose of the noise vector, and ε_i is a normally distributed random variable with mean zero and variance σ^2, then the regression weights determined from the data are

$$\hat{\beta} = \left[X^t V^{-1} X\right]^{-1} \left[X^t V^{-1} Y\right] , \tag{3}$$

where -1 denotes matrix inversion and the objective analysis may be accomplished by

$$\hat{Y} = X\hat{\beta} . \tag{4}$$

See Draper and Smith[6] for details.

The kth, lth element of the matrix $[X^t V^{-1} X]$ is computed by

$$\left[X^t V^{-1} X\right]_{kl} = \sum_i^N \sum_j^N X_{ik} X_{jl} V_{ij}^{-1} , \tag{5}$$

and the kth element of the vector $[X^t V^{-1} Y]$ is computed by

$$\left[X^t V^{-1} Y\right]_k = \sum_i^N \sum_j^N X_{ik} Y_j V_{ij}^{-1} . \tag{6}$$

The covariance structure function, cov(XX), is determined from the historical data set for all possible kth, lth elements of $[X^t V^{-1} X]$ and for all

---

[6]N. R. Draper and H. Smith, 1966, Applied Regression Analysis, Wiley Press, 401 pp

possible kth elements of $[X^t V^{-1} Y]$, and is expressed in terms of a mathematical model. The signal plus noise covariance can be computed from this modeled structure for any kth, lth element required, within the limits of the model itself.

$\Delta t = t_2 - t_1$

X_1 = position (E-W) of variable 1

X_2 = position (E-W) of variable 2

Y_1 = position (N-S) of variable 1

Y_2 = position (N-S) of variable 2

t_1 = observation time of variable 1

t_2 = observation time of variable 2

The decision variables (NLP estimated parameters) are as follows:

A = modeled lag zero correlation coefficient.

σ_x, σ_y, σ_t = modeled measures of storm size in space and time.

α = a measure of ellipticity.

C_x and C_y = modeled speeds toward the east and north (positive), respectively (figure 3).

Crawford's[7] NLP algorithm minimizes an objective function, subject to mathematical constraints. The algorithm adjusts the values of the variables until any minor change in these variables results in an improvement of the objective function of less than some small preset value. The algorithm thus converges upon values of the variables which are as good as or better than any nearby values.

In the above formulation, variables 1 and 2 were both IR or visible, thus producing an autocovariance function.

SYNOPTIC SITUATION

The first case used to test the objective analysis procedures occurred on 20-21 May 1977 over the south-central United States (see appendix for map series). The synoptic situation on 19 May at 1200Z showed a high pressure system centered over Kentucky with a low pressure over North Dakota. A

---

[7]K. C. Crawford, 1977, "The Design of a Multivariate Mesoscale Field Experiment," PhD Dissertation, University of Oklahoma, Department of Meteorology

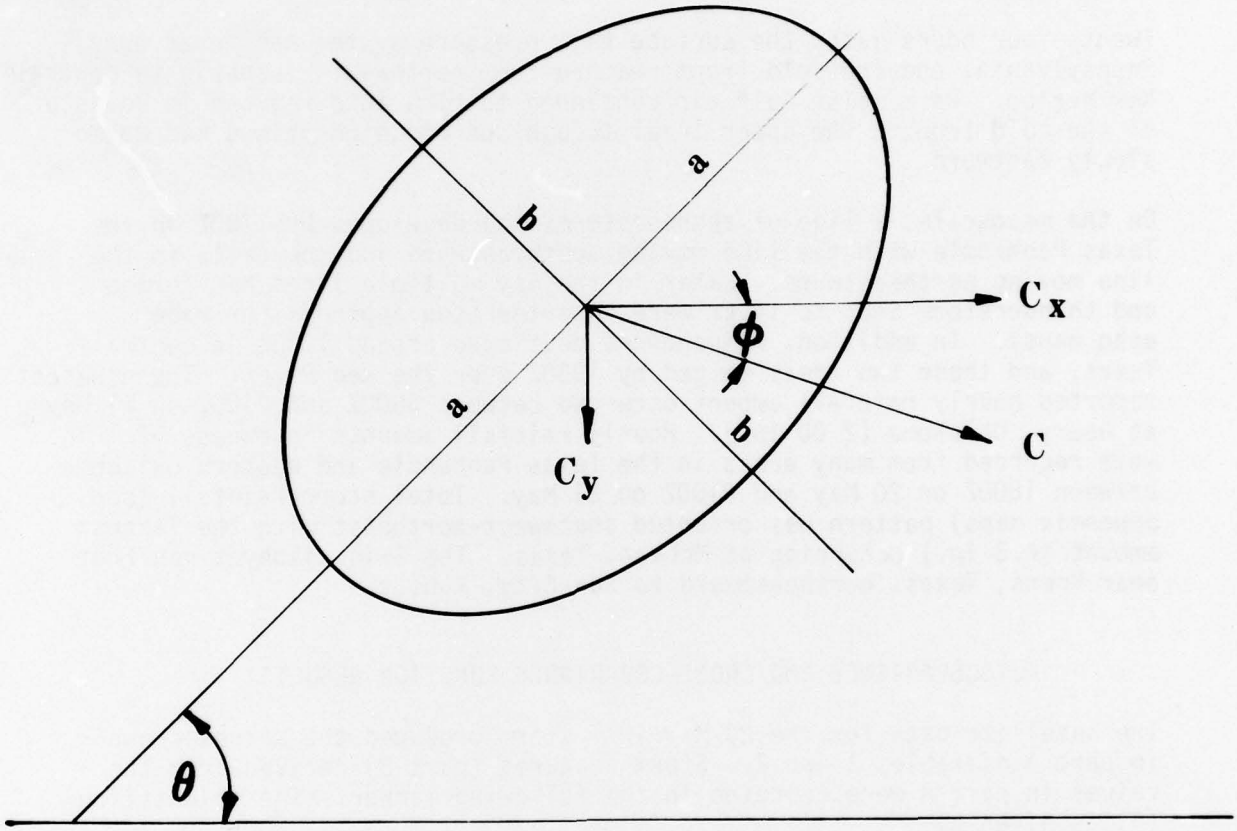

Figure 3: Cloud top characteristics for one portion of the storm, lifetime deduced from the modelled covariance function. a=major axis, b=minor axis, θ =orientation, c_x = eastward speed of storm, c_y = southward speed of storm, ϕ = direction of movement

cold front extended from this low pressure system southwestward through South Dakota, Nebraska, western Kansas, and Oklahoma into the Texas Panhandle. Flow in advance of the front was southerly, bringing warm moist air from the Gulf of Mexico in the Great Plains. Surface temperatures in advance of the front ranged from the lower 70's in North Texas to the lower 60's in North Dakota with dew point temperatures ranging from the mid 60's to the mid 50's.

Upper airflow at 700 mb on the 19th was characterized by a ridge over the eastern portion of the United States, while a trough spanned the area from Idaho through eastern Nevada into southern California.

Twenty-four hours later the surface high pressure system had moved over Pennsylvania, and the cold front reached from northwest Wisconsin to central New Mexico. Warm moist Gulf air continued to flow into regions in advance of the cold front. The upper level trough and ridge positions had moved slowly eastward.

On the mesoscale, a line of thunderstorms had developed by 1700Z in the Texas Panhandle with the line moving southeastward and the cells in the line moving northeastward. Later in the day multiple lines had formed and thunderstorm tops to 14 km were reported (see appendix for radar echo maps). In addition, rainshowers developed around 1630Z in central Texas, and these two areas merged by 1930Z over the Red River. The greatest reported hourly rainfall amount occurred between 0000Z and 0100Z on 21 May at Geary, Oklahoma (2.00 in.). Hourly rainfall amounts in excess of 1 in. were recorded from many areas in the Texas Panhandle and western Oklahoma between 1800Z on 20 May and 0100Z on 21 May. Total storm rainfall (see appendix maps) pattern was oriented southwest-northeast with the largest amount (4.3 in.) occurring at McLean, Texas. The 3-in. isohyet ran from near Kress, Texas, northeastward to Sun City, Kansas.

AUTOCOVARIANCE AND CROSS-COVARIANCE FUNCTION RESULTS

The satellite data for the 20 May 1977 storm produced the values shown in part A of tables 1 and 2. Storm features (part B) derived from the values in part A were computed in the following manner. The orientation (θ) is given by

$$\theta = (1/2)\ \text{ARCTAN}\left[2\alpha\sigma_x\ \sigma_y/(\sigma_x^2 - \sigma_y^2)\right] \qquad (8)$$

The major axis(a) is computed from equation (9)

$$a^2 = \sigma_x^2 \cos^2\theta + \sigma_y^2 \sin^2\theta + 2\alpha\sigma_x\sigma_y \sin\theta \cos\theta\ . \qquad (9)$$

TABLE 1. INFRARED DATA (THRESHOLD = -30°C)

Part A					Part B							
σ_x (km)	σ_y (km)	α	ρ	Time(Z)	θ (deg)	a (km)	b (km)	Area $km^2 \times 10^3$	Shape a/b	Direction (deg)	Speed (km/hr)	S/N
199	259	0.09	0.61	1800 - 1845	54	249	211	165	1.18	220	81	0.59
197	272	0.20	0.62	1815 - 1854	61	274	195	168	1.41	223	62	0.62
195	300	0.25	0.63	1830 - 1915	60	299	196	184	1.53	229	58	0.66
195	328	0.26	0.65	1845 - 1930	58	321	206	208	1.56	229	72	0.73
191	354	0.25	0.66	1854 - 1945	55	335	223	235	1.50	234	67	0.77
191	369	0.20	0.66	1915 - 2000	53	337	243	257	1.39	249	50	0.77
197	365	0.14	0.66	1930 - 2015	51	325	258	263	1.26	252	50	0.77
211	362	0.01	0.65	1945 - 2030	45	298	295	276	1.01	239	67	0.73
226	354	-0.14	0.64	2000 - 2045	8	356	222	248	1.60	226	82	0.69
242	352	-0.23	0.63	2015 - 2100	15	360	231	261	1.56	222	99	0.66
262	356	-0.25	0.63	2030 - 2115	19	367	246	284	1.49	220	92	0.66
272	379	-0.23	0.61	2045 - 2130	17	389	258	315	1.51	221	92	0.59
295	452	-0.24	0.59	2100 - 2145	14	461	281	407	1.64	207	91	0.53

TABLE 2. VISIBLE DATA 20 MAY 1977

Part A					Part B							
σ_x (km)	σ_y (km)	α	ρ	Time(Z)	θ (deg)	a (km)	b (km)	Area $km^2 \times 10^3$	Shape a/b	Direction (deg)	Speed (km/hr)	S/N
224	223	0.51	0.60	1800 - 1845	45	275	156	135	1.76	200	94	0.56
214	224	0.58	0.61	1815 - 1854	47	275	142	123	1.94	200	83	0.59
216	235	0.58	0.60	1830 - 1915	49	284	146	130	1.95	202	95	0.56
221	249	0.59	0.60	1845 - 1930	51	298	149	139	2.00	201	95	0.56
225	255	0.57	0.64	1854 - 1945	51	302	156	148	1.94	197	102	0.69
228	256	0.50	0.67	1915 - 2000	52	298	170	159	1.75	204	75	0.81
228	253	0.43	0.68	1930 - 2015	52	289	180	163	1.61	205	62	0.86
221	244	0.37	0.68	1945 - 2030	53	274	183	158	1.50	206	67	0.86
216	238	0.32	0.67	2000 - 2045	53	262	186	153	1.41	198	70	0.81
219	230	0.31	0.64	2015 - 2100	49	257	186	150	1.38	206	71	0.69
231	207	0.32	0.63	2030 - 2115	36	254	179	143	1.42	213	64	0.66
253	181	0.33	0.61	2045 - 2130	22	265	163	136	1.63	227	68	0.59
273	153	0.34	0.58	2100 - 2145	15	280	140	123	2.00	224	64	0.51

The minor axis(b) is given by

$$b^2 = \sigma_x^2 \sin^2 \theta + \sigma_y^2 \cos^2 \theta - 2\alpha\sigma_x\sigma_y \sin \theta \cos \theta \ . \qquad (10)$$

The area is computed from equation (11)

$$A = \pi(a)(b) \ ; \qquad (11)$$

and the shape by

$$s = a/b \ ; \qquad (12)$$

and the signal to noise ratio (SNR) can be inferred from the modeled lag zero correlation coefficient as follows (equation (13))

$$SNR = \frac{\rho^2}{1 - \rho^2} \qquad (13)$$

Also, C is the speed of movement of the storm and ϕ is the direction of movement.

The derived storm characteristics are conservative and stable over the 1800Z to 2145Z time period. The change in orientation shown at 2000Z was due to the merging of a small cell with the convective complex (see appendix for radar coverage). The colder IR temperatures became numerous in the southern portion of the storm during the merger, thus forcing the orientation angle around to a more easterly direction; however, the direction of movement (ϕ) of the total storm remained about the same. Figures 4 and 5 show a plot of some of the significant parameters of the convective complex. Weather radar reports from Lubbock, Texas, indicated average cell movements of 30 to 35 knots (55 to 64 km/hr) with a direction of 230 at 1800Z. Maximum observed cell speed by weather radar was 50 knots (91 km/hr) from 230. Later in the day (2030Z), the Oklahoma City weather radar reported cells moving at about 25 to 30 knots (46 to 55 km/hr) from 230 to 240 degrees azimuth. A maximum speed of 35 knots with an azimuth of 230 was also recorded.

The computed storm orientation (θ) agrees well with the surface rainfall pattern up until time of cell merger. (See appendix for rainfall analysis.) The area shown in tables 1 and 2 indicates that the visible cloud top is somewhat smaller and oriented a little differently than the IR cloud top. The overshooting tops seen in the visible data (figure 6) are pronounced and tend to line up along the direction of motion. These features tend to make the covariance algorithm deduce a smaller system.

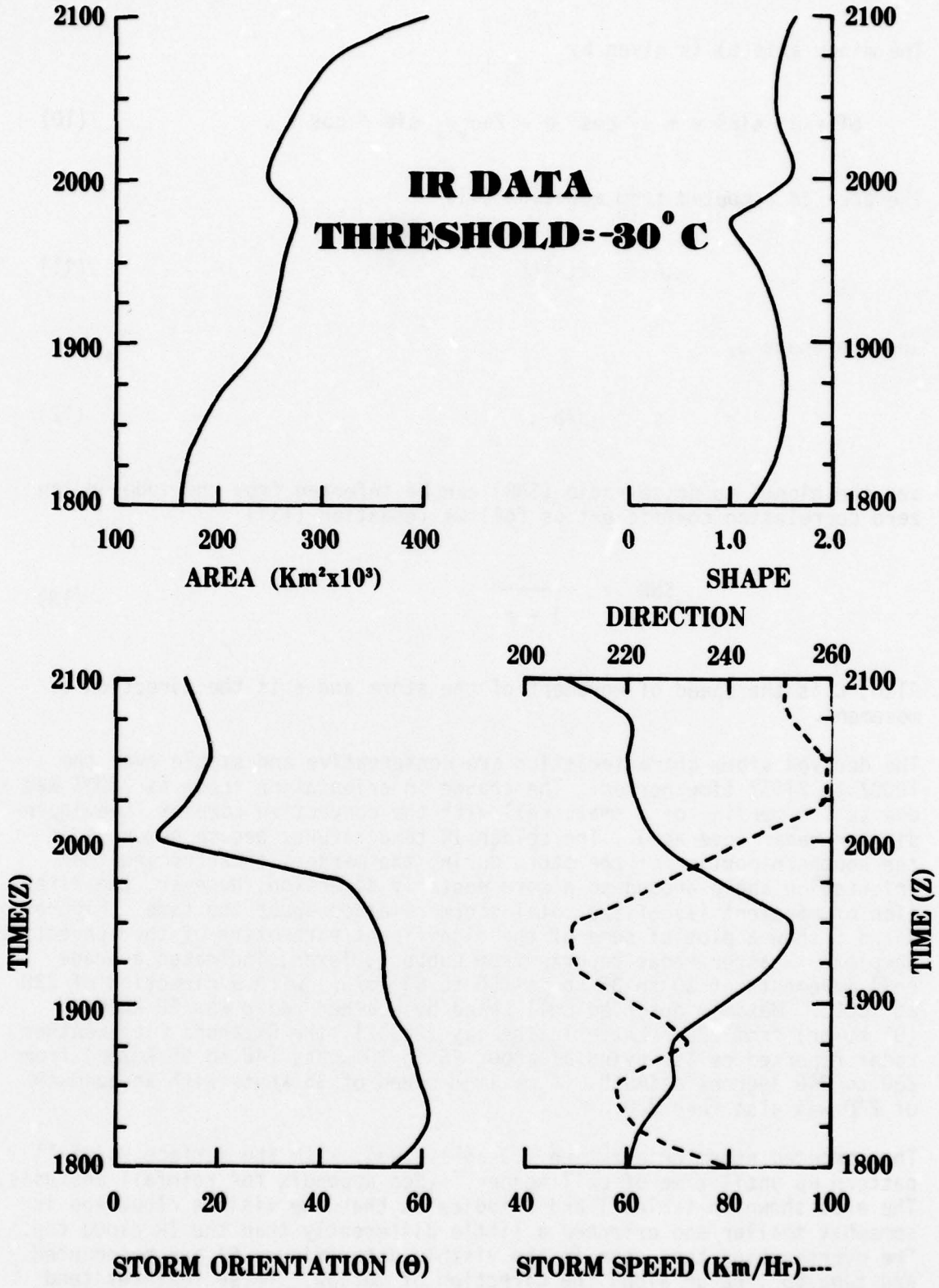

Figure 4. Significant parameters of convective complex. IR threshold data = -30°C.

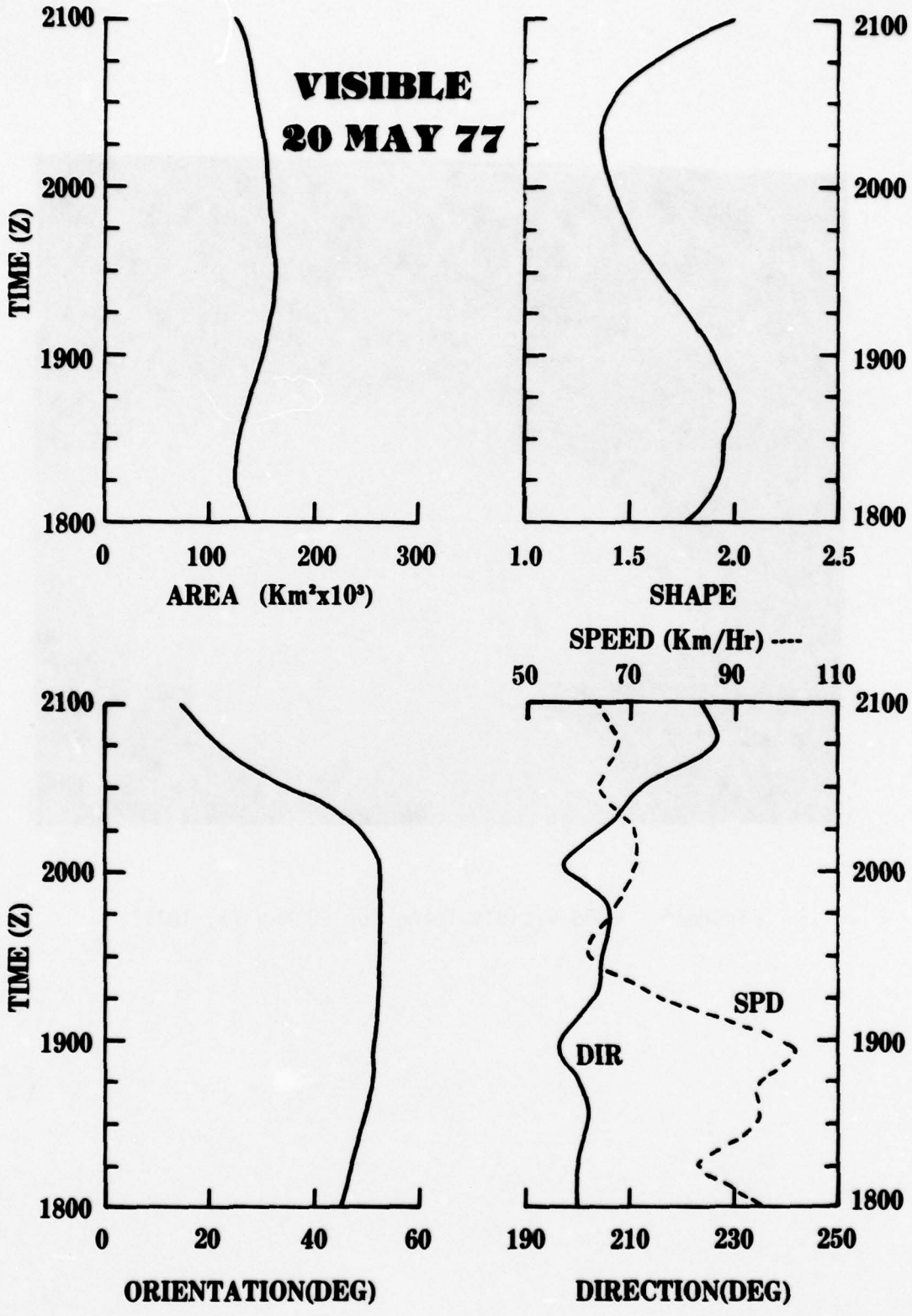

Figure 5. Significant parameters of convective complex. Visible data 20 May 77.

Figure 6. GOES visible image for 20 May 77, 1815Z.

The SNR increased and then decreased with time. The convective complex evolved during the period of analysis from a smooth and well-defined ellipse up until the time of cell merger. Then the system became a rather flat and ragged composite of anvils produced by several embedded cells (figure 7). The SNR could be anticipated to drop to very small values as the system ceased to produce new active rain cells.

Several inferences can be made from the results of this study, namely: (1) cloud top morphology of convective complexes as deduced by using the space-time covariance analysis technique is sufficiently conservative to suggest that predictions made for periods of about 1 to 2 hours could show significant skill; (2) these predictions can be objective and automated; and (3) rainfall location, movement, and intensity can be associated with cloud top features of such weather systems.

All the statistics required to perform the analysis of the GOES data are contained in the cross-covariance functions derived from the data sets. The first step in modeling these functions is to obtain "raw," discrete covariance estimates by lagging each field with respect to itself in space and time. To cover the entire storm and yet preserve an adequate space-time resolution, the raw covariance matrices were of order 9 by 9 in space and 4 in time. The category sizes or resolution were 70 km east-west, 70 km north-south and 15 minutes in time. The product pairs and the raw covariance matrices for selected times are presented in the appendix.

The raw covariance matrices are normalized to give raw correlation matrices. Equation (7) was fitted to the raw correlation matrices by using a non-linear program (NLP) algorithm developed by Crawford.[7]

$$\begin{aligned} \text{Cov}\,(X_1X_2) = A * \exp\Big\{\Big[-1/2(1-\alpha^2)\Big]\ \Big[(\Delta X/\sigma_x)^2 \\ - 2\alpha(\Delta X/\sigma_x)\,(\Delta Y/\sigma_y) + (\Delta Y/\sigma_y)^2\Big] \\ - (1/2)\,(\Delta t/\sigma_t)^2\Big\} * \text{Cos}\Big\{(\pi/2)\Big[(\Delta X/\sigma_x)^2 \\ - 2\alpha(\Delta X/\sigma_x)\,(\Delta Y/\sigma_y) + (\Delta Y/\sigma_y)^2 + (\Delta t/\sigma_t)^2\Big]^{1/2}\Big\} \end{aligned} \qquad (7)$$

[7]K. C. Crawford, 1977, "The Design of a Multivariate Mesoscale Field Experiment," PhD Dissertation, University of Oklahoma, Department of Meteorology

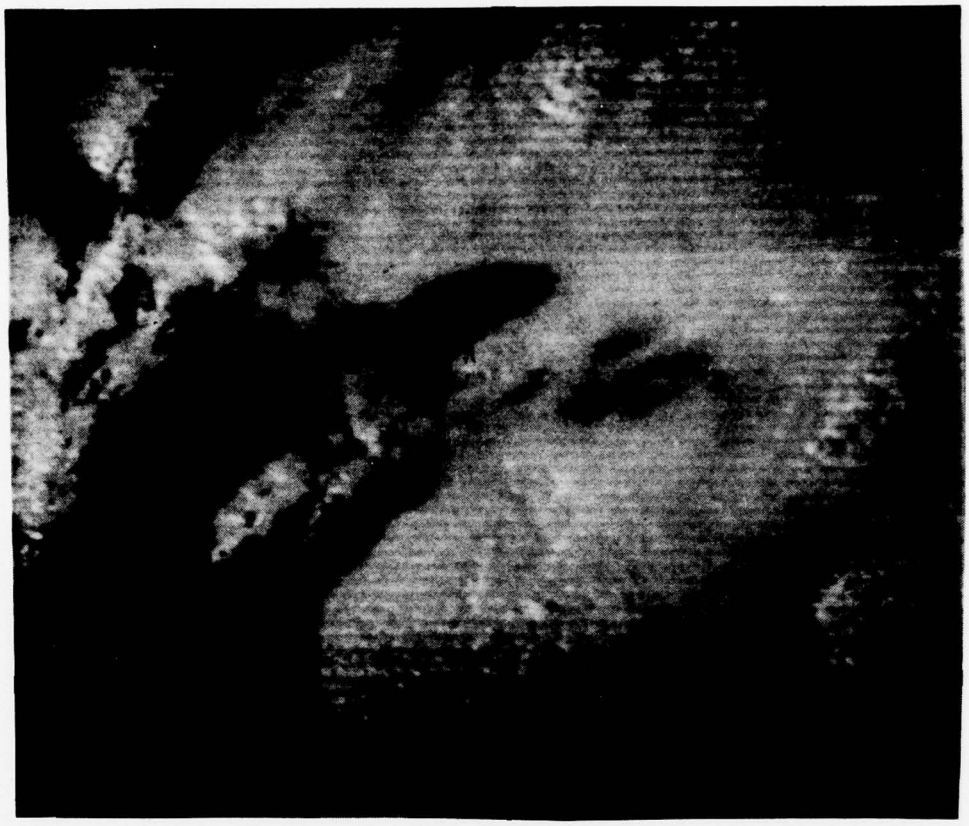

Figure 7. GOES visible image for 20 May 77, 2115Z.

where

$$\Delta X = (X_2 - X_1) - C_x t - X_o$$

$$\Delta Y = (Y_2 - Y_1) - C_y t - Y_o$$

RAIN GAGE - SATELLITE DATA COMPARISON

The procedures in the previous action showed that an ellipse can be fitted to a convective complex and useful parameters can be derived from the auto-covariance and cross-covariance functions. However, if an analysis system is to operate in a real-time mode, the above procedures require too much computer time for operational purposes.

An ellipse fitting routine* was developed for the AMAS image processor which allows an ellipse, similar in configuration to the ones in the previous section, to be fitted to the convective complex temperature patterns in a few seconds of computer time. Successive images can be averaged or displayed individually as the analyst desires. This system also allows image overlay of other data. Using the navigation system, one can take each line-element location on the image and transform it into latitude and longitude; one can transform earth-located information into the satellite coordinate system or vice-versa for proper comparison of the data. This system permits new insight into the physical mechanisms occurring during the rainfall process and demonstrates where efforts should be made in further studies.

Rainfall data for the 20 May 1977 period was available at hourly intervals from some stations and on a daily total basis from other stations. Figures 8, 9, 10, and 11 compare the hourly rainfall totals for 1900Z, 2000Z, 2100Z, and 2200Z with the fitted ellipses which correspond to the -63°C, -65°C, and -67°C IR temperatures averaged for the half-hour and hourly values ending on the hour. Since the available satellite data did not span a 24-hour period, no comparison was made with the total rainfall pattern. The greatest amounts of recorded rainfall fell within the -67°C fitted ellipse. All but two rainfall events greater than 0.50 in. fell within the -67°C ellipse. However one station (within the -67°C ellipse) did not report any rain during the 4-hr time period. The -63°C fitted ellipse encompassed most of the significant (> 0.50 in./hr) rainfall events. Only one event fell outside this ellipse. More rain usually fell after mergers of -67°C contour areas.

---

*J. Marvin, Physical Science Laboratory, New Mexico State University, personal communication

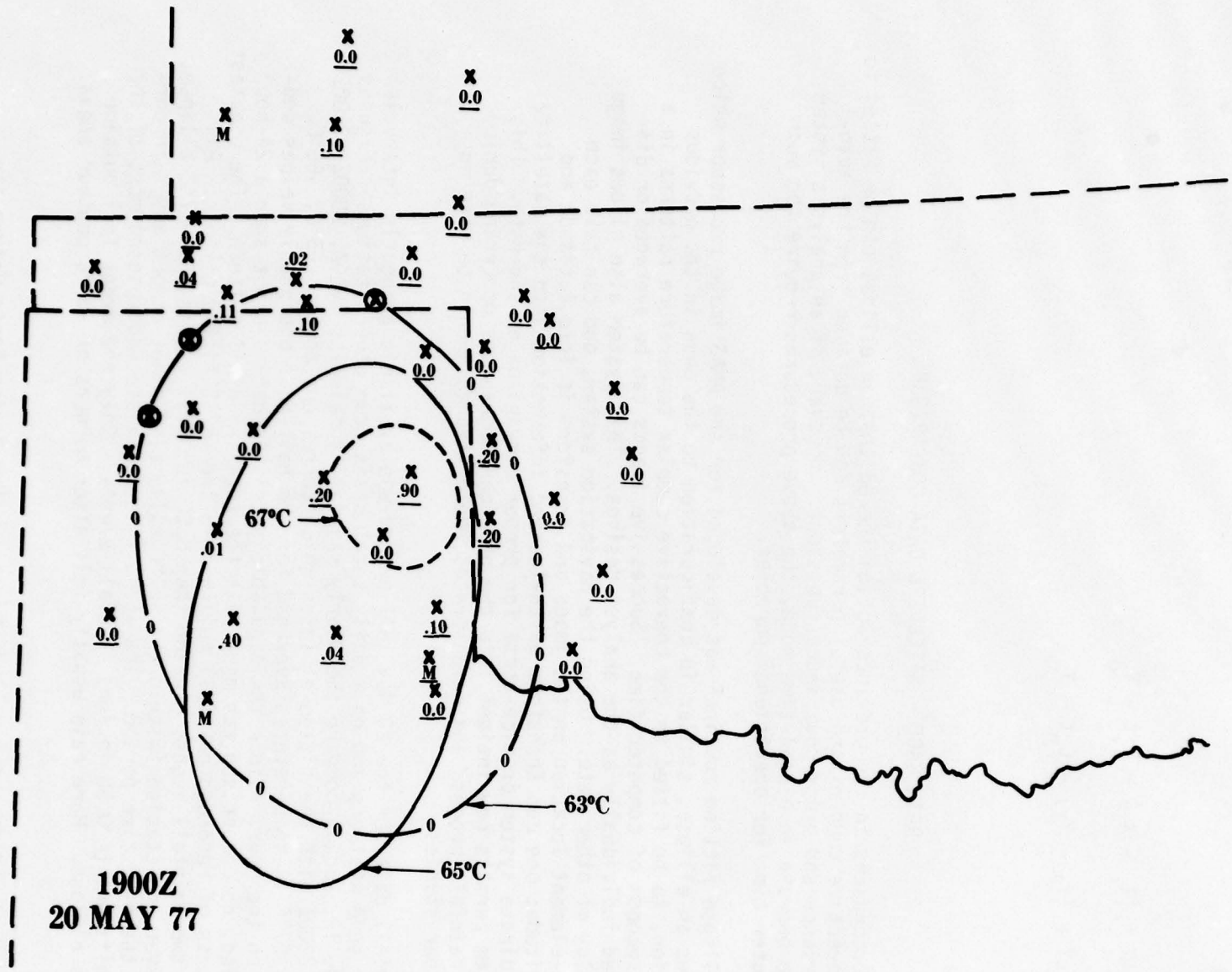

Figure 8. Hourly rainfall rate, 1900Z, 20 May 77, compared with fitted ellipses.

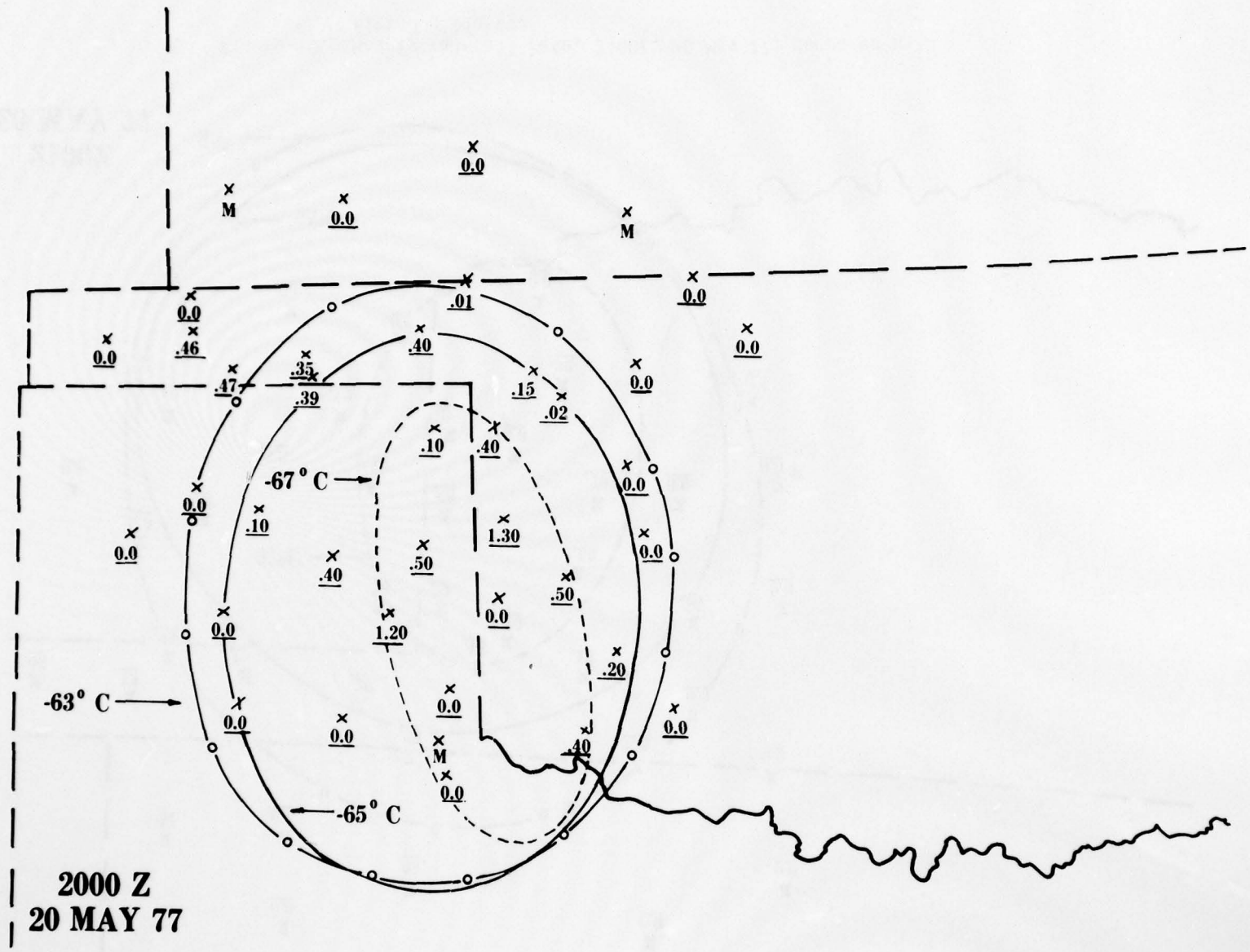

Figure 9. Hourly rainfall rate, 2000Z, 20 May 77, compared with fitted ellipses.

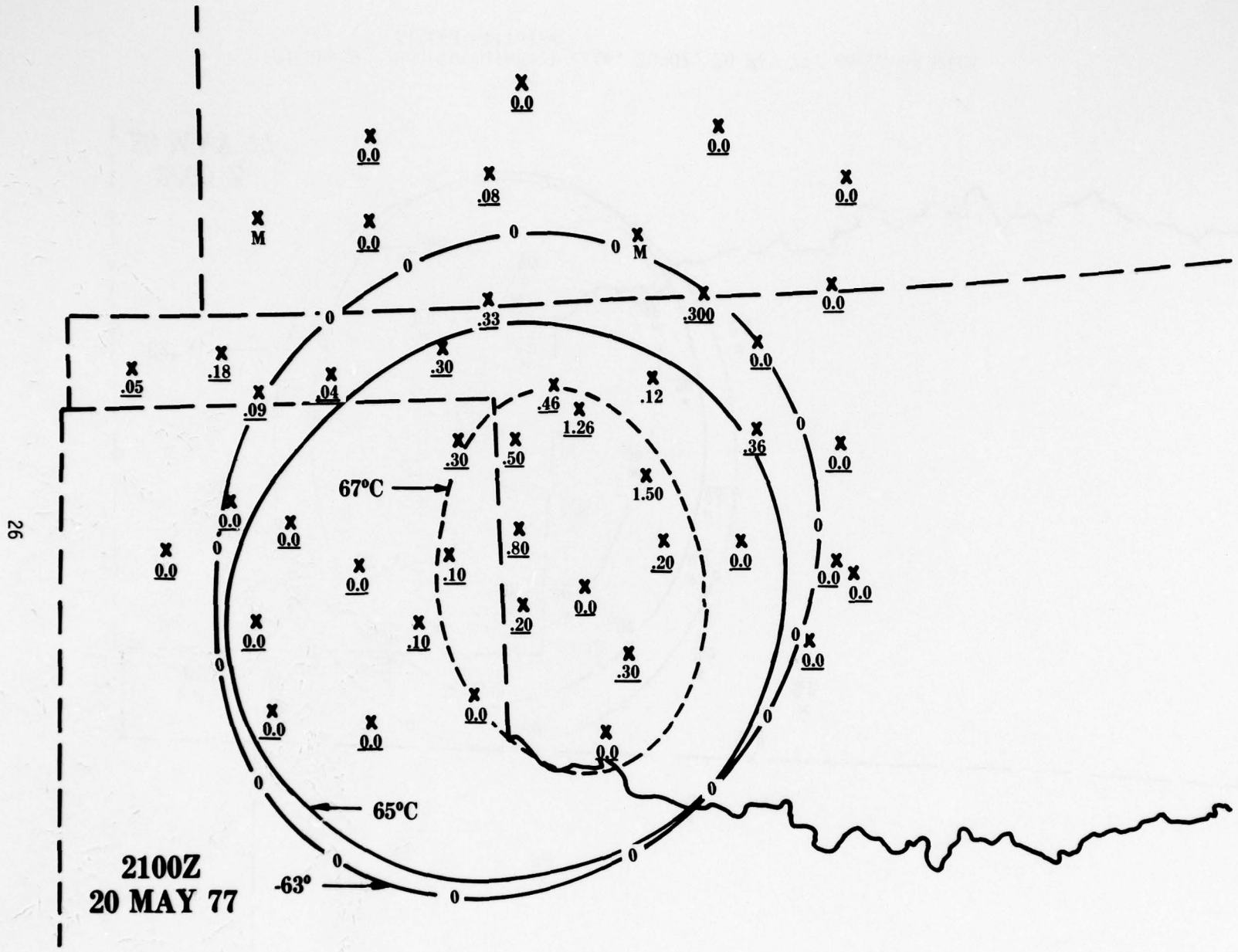

Figure 10. Hourly rainfall rate, 2100Z, 20 May 77, compared with fitted ellipses.

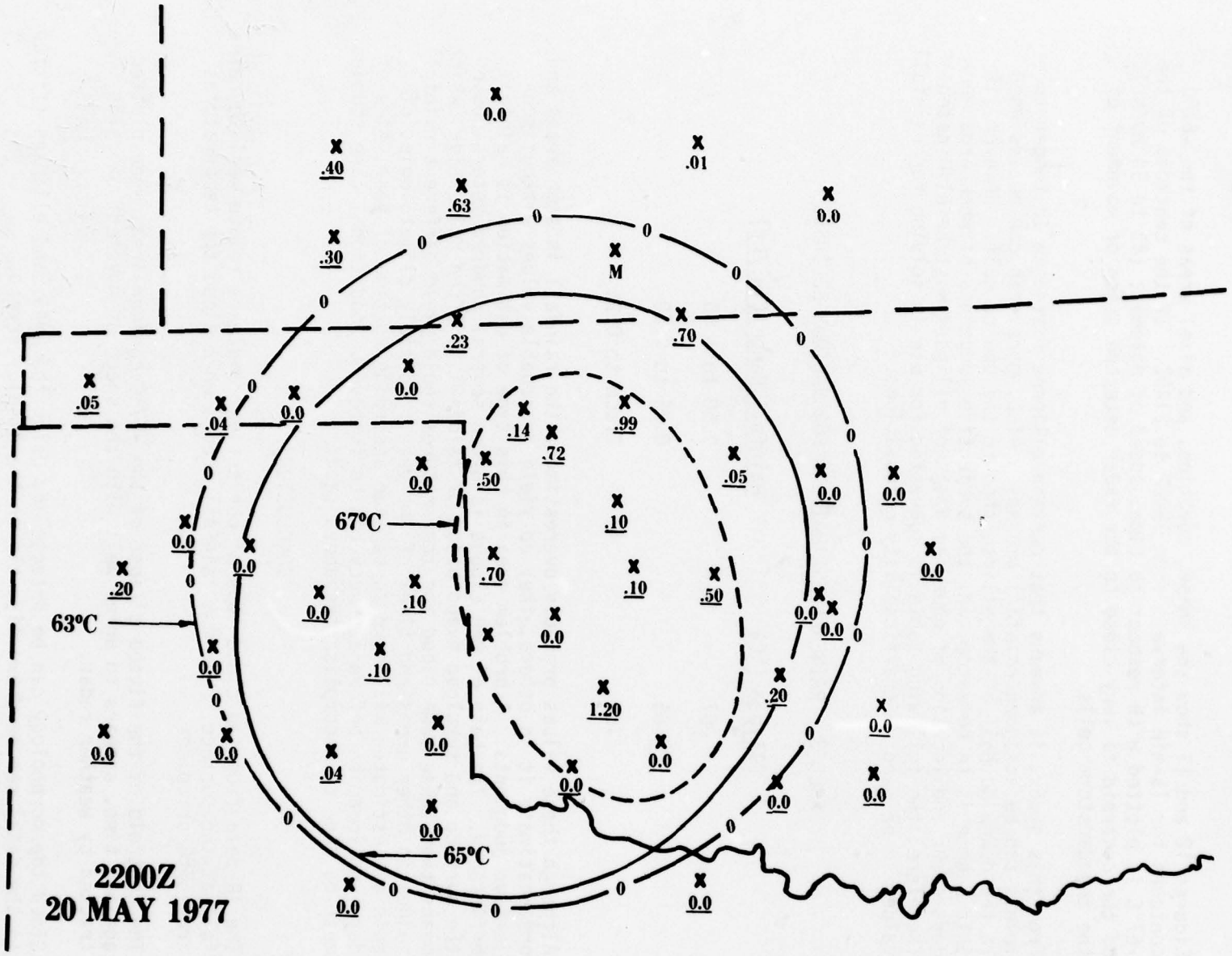

Figure 11. Hourly rainfall rate, 2200Z, 20 May 77, compared with fitted ellipses.

Figures 12 and 13 show the shape, position, and pixel areas of the -67°C contours for 15-min intervals from 1800Z to 2145Z. If the centroid of the -67°C is plotted with respect to time, speed of movement (43 to 54 km/hr) of the centroid is very close to the radar detected speed of movement of the thunderstorm cells.

From this study, it appears that certain ellipses fitted to IR temperature levels can be assigned rainfall amounts. Also, more rain can be assigned to the downwind half of the ellipse than to the upwind half. However, if this scheme is to be automated, the subjective judgments of when area mergers occur and location of downwind areas of ellipses must be eliminated. Therefore, the following table is suggested for use in solving for rainfall values to be used in trafficability calculations.

TABLE 3. RAINFALL ESTIMATIONS FOR VARIOUS ELLIPSES

Ellipse (°C)	Rainfall Range (in./hr)
-67	0.50 to 1.50
-65	0.25 to 0.50
-63	Trace to 0.25

Although these values probably overestimate the rainfall in some areas and underestimate it in others, they do yield reasonable values without subjective judgments. A problem area in this type of estimation is rainfall efficiency. The base of the clouds is often several hundred meters above the surface and subcloud evaporation of rainfall is often quite high, which means that these same cloud top temperatures could yield different rainfall values in other areas and times of the year. Possibly climatologies of rainfall estimates will have to be made according to time of year, time of day, and location before accuracy can be improved. Additional case studies must be done to accomplish the above task.

CONCLUSIONS

The IR data from the cloud tops of convective complexes relate well to rainfall at the surface. Maximum rainfall occurs when cloud top temperatures are -67°C or colder.

The centroid of the fitted ellipse of the -67°C contour area, when plotted against time, appears to agree well with the speed of movement of cells tracked by weather radar.

Cloud top morphology can be detected by using the AMAS, and ellipses (fitted to the data) can be drawn directly on the display screen.

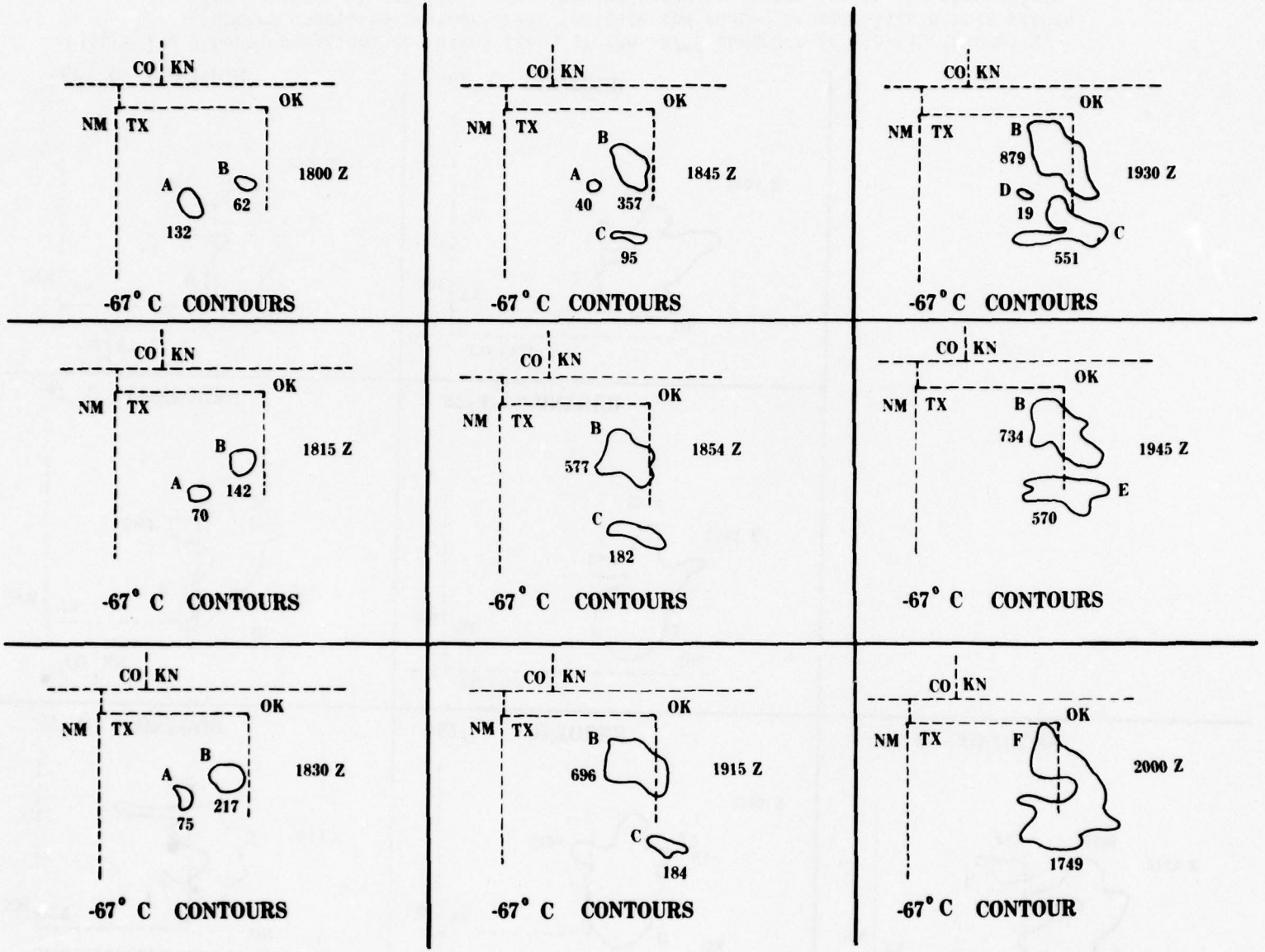

Figure 12. Shape, position, and pixel areas of the -67°C contours for 15-min intervals. Numbers under the contour areas indicate the number of satellite pixels within the contour. Mergers of areas are indicated by letter designator change from one time period to another.

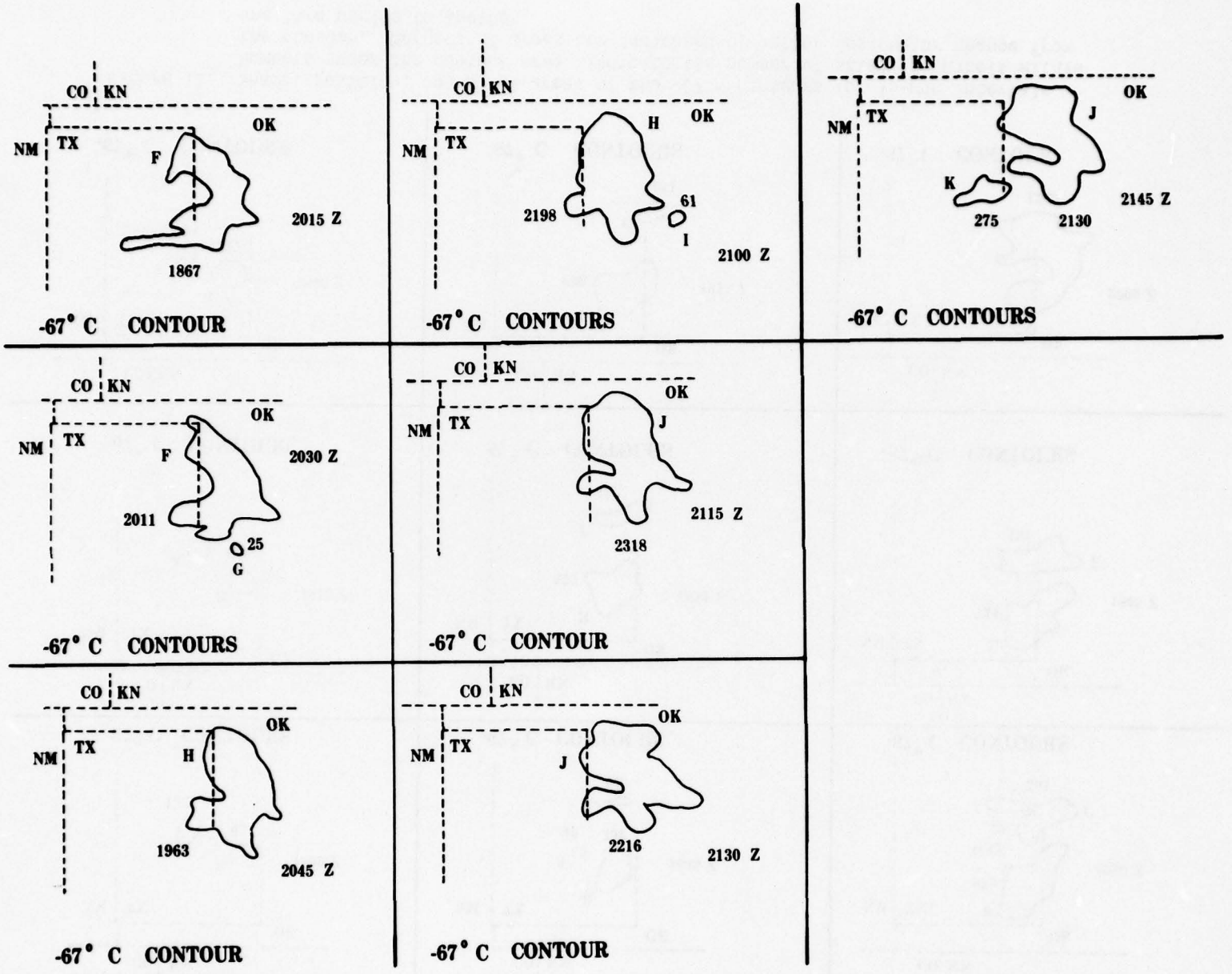

Figure 13. Shape, position, and pixel areas of the -67°C contours for 15-min intervals. Numbers under the contour areas indicate the number of satellite pixels within the contour. Mergers of areas are indicated by letter designator change from one time period to another.

Convective complex movements and areal expansion rates can be predicted by using past positions of the centroid and areas of a fitted ellipse and extrapolation techniques.

REFERENCES

1. Scofield, R. A., and V. J. Oliver, 1977, "A Scheme for Estimating Convective Rainfall from Satellite Imagery," NOAA Technical Memo NESS 86.

2. Eddy, A., and L. Hembree, 1977, "Space-Time Sampling from SMS Satellite Data Required to Define Convective Storms," Final Report, Contract DAAG29-76-D-0100. US Army Research Office.

3. Phillips, D. R., and E. Smith, 1974, "Geosynchronous Satellite Navigation Model," Internal Report, University of Wisconsin Space Sciences and Engineering Center.

4. Billingsley, J., J. Chen, C. Mottershead, A. Bellian, and T. DeMott, 1977, "AOIPS METPAK, a Meteorological Data Processing System," Computer Science Corporation Report CSC/SD-77/6084.

5. Eddy, A., 1973, "The Objective Analysis of Atmospheric Structure," J Meteorol Soc Japan, 51:450-57.

6. Draper, N. R., and H. Smith, 1966, Applied Regression Analysis, Wiley Press, 401 pp.

7. Crawford, K. C., 1977, "The Design of a Multivariate Mesoscale Field Experiment," PhD Dissertation, University of Oklahoma, Department of Meteorology.

APPENDIX

GENERAL REFERENCE MAPS FOR 20 MAY 1977

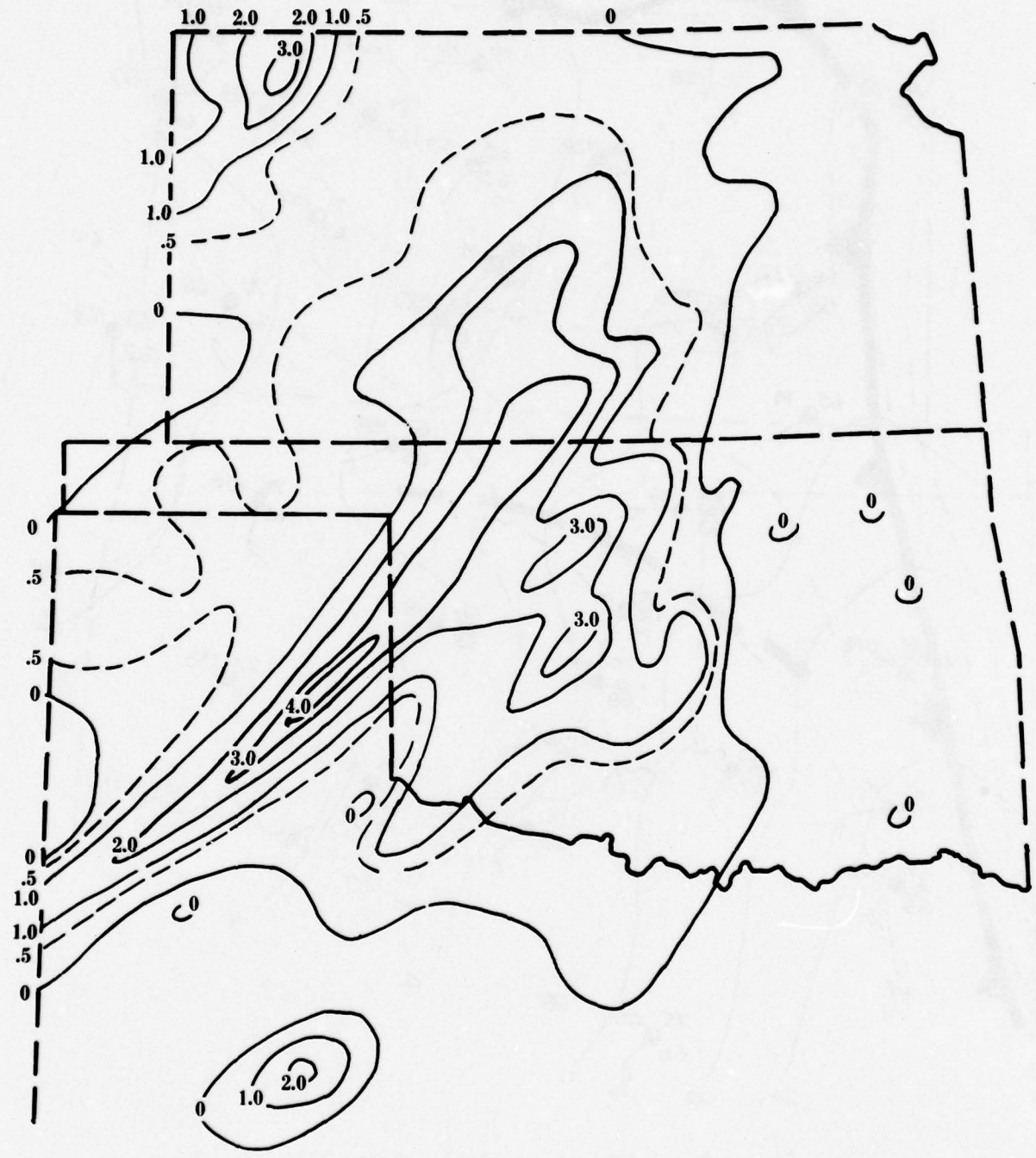

Figure A-1. Total Precipitation 1600Z 20 May 77 through 0200Z 21 May 77.

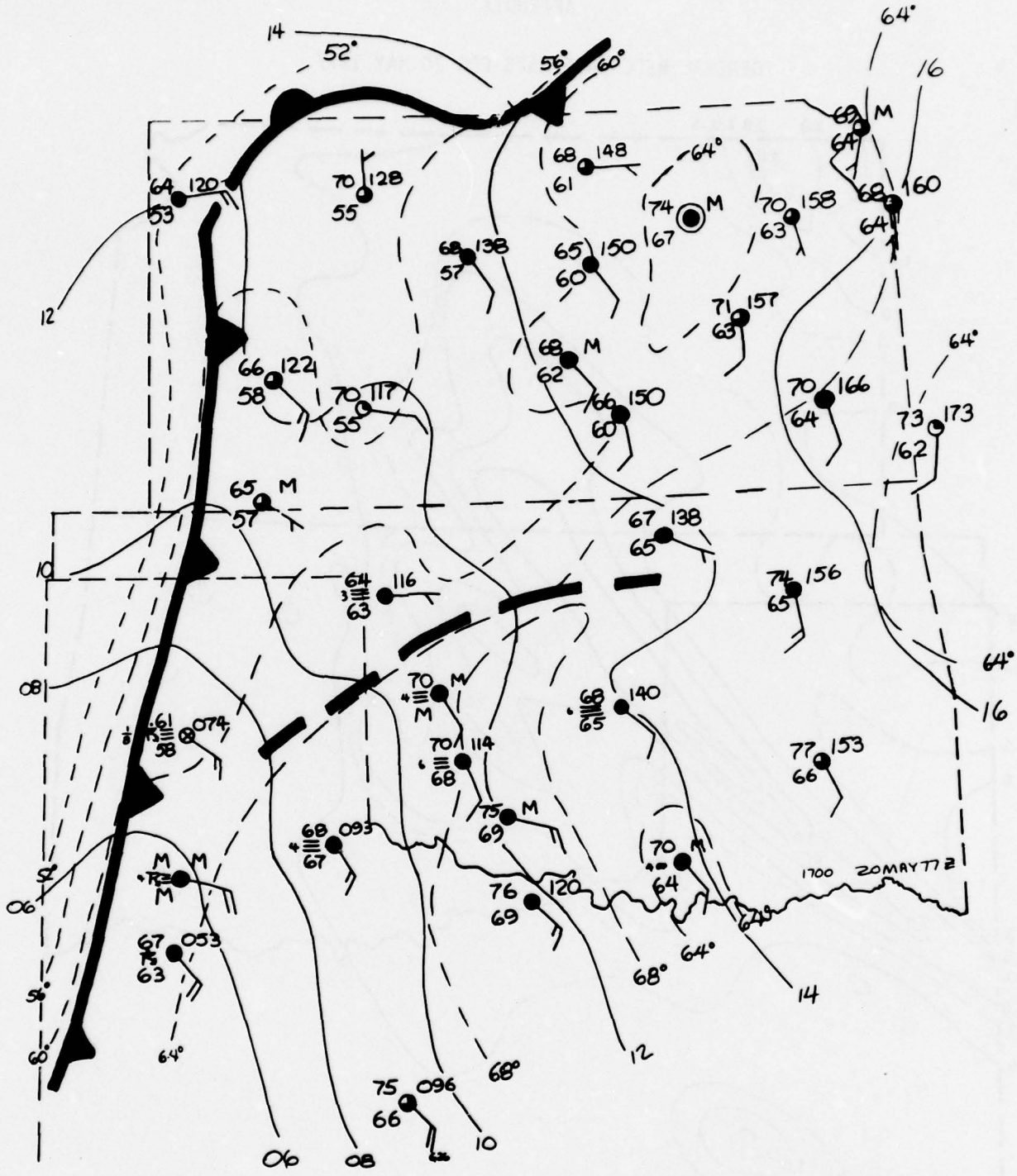

Figure A-2. Surface at 17007, 20 May 77.

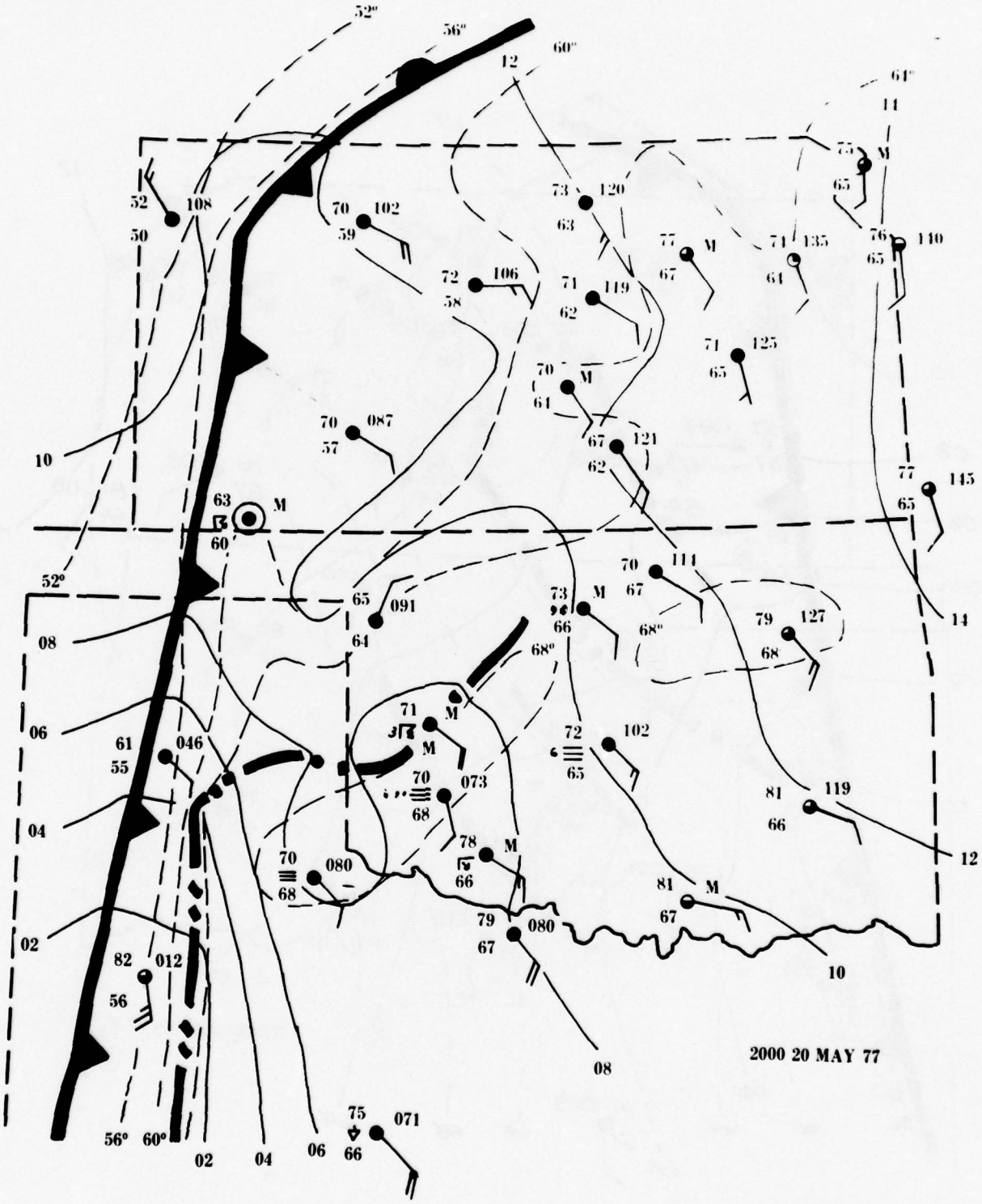

Figure A-3. Surface at 2000Z, 20 May 77.

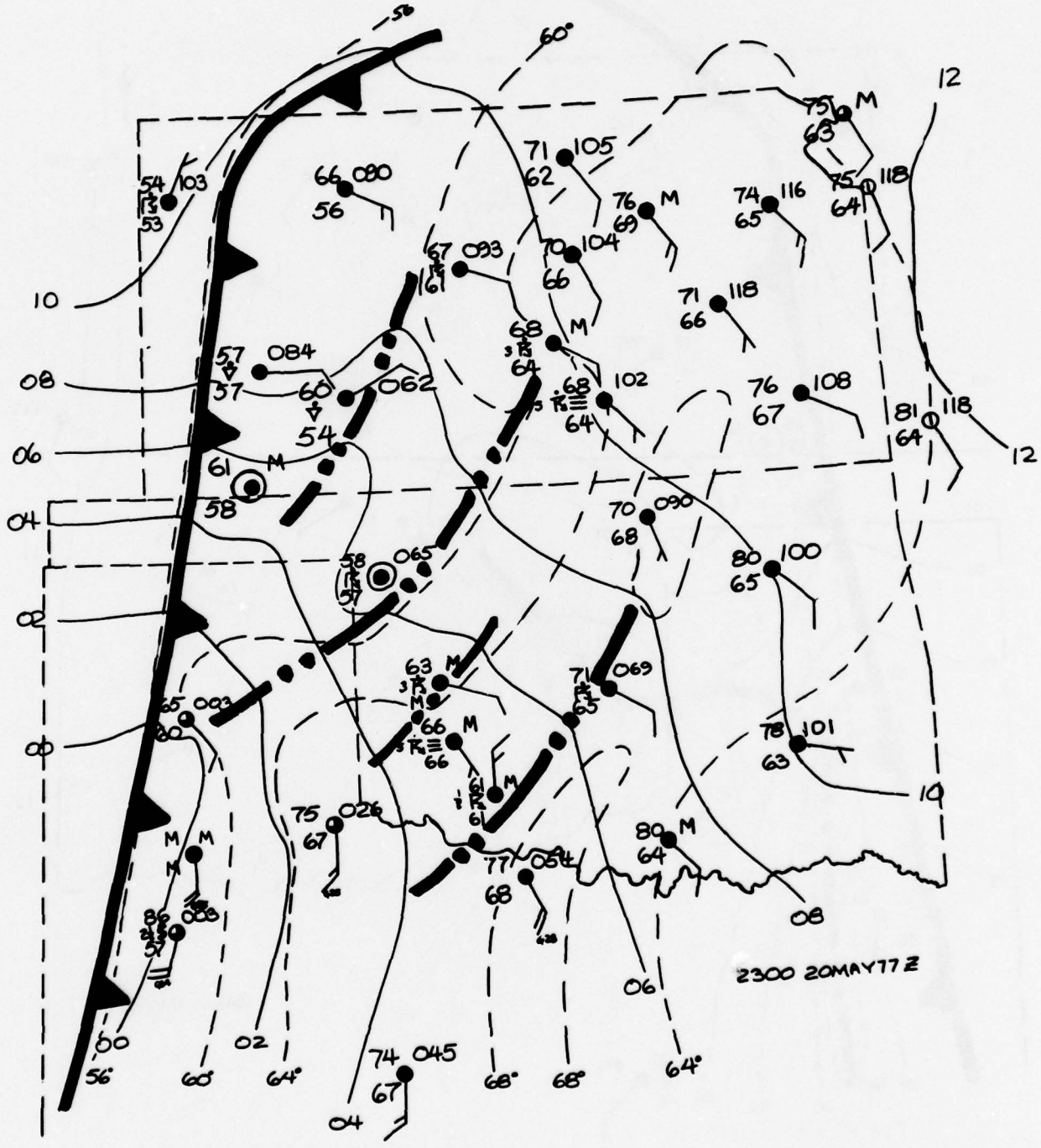

Figure A-4. Surface at 2300Z, 20 May 77.

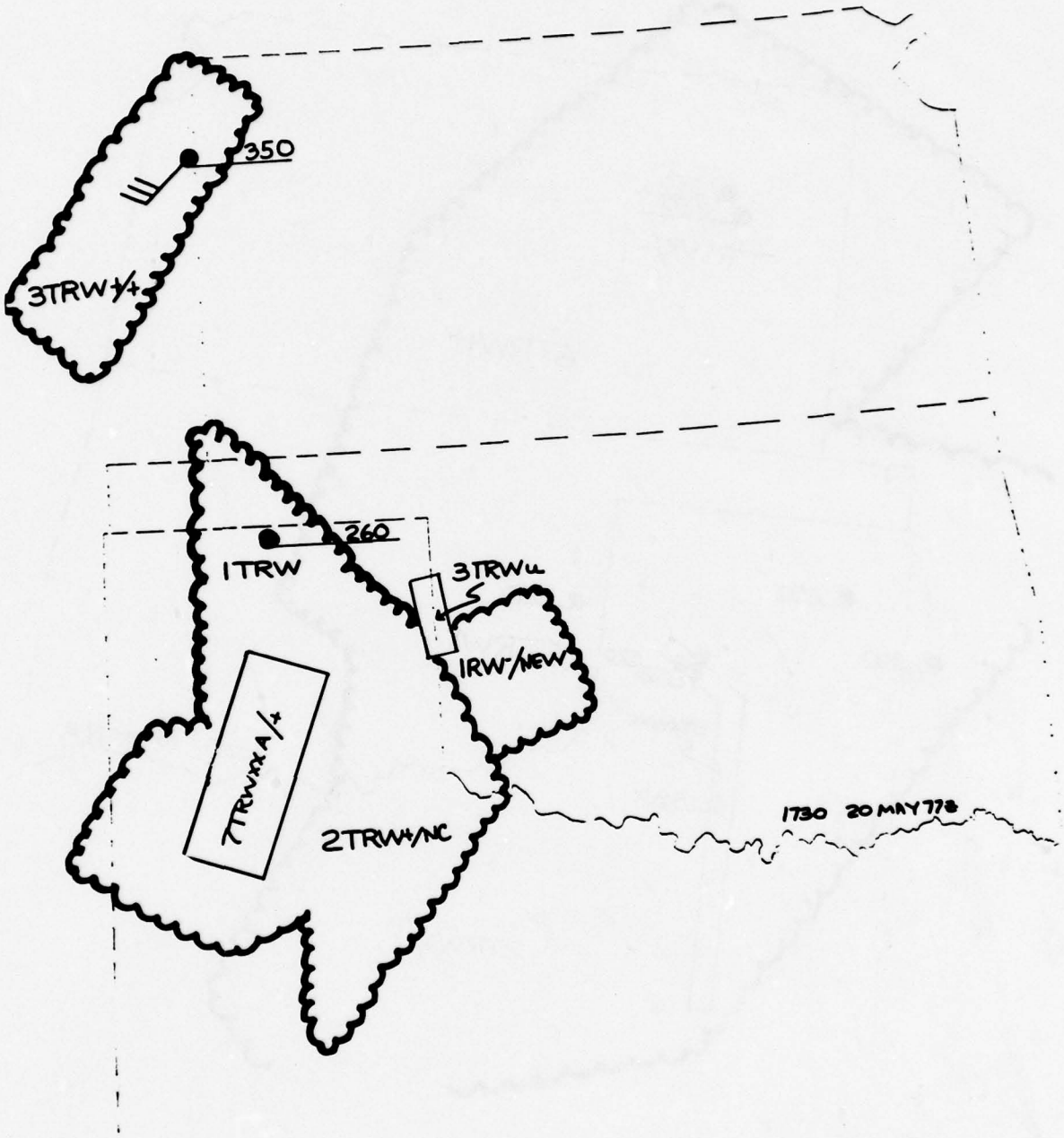

Figure A-5. Composite radar echoes for 1730Z, 20 May 77.

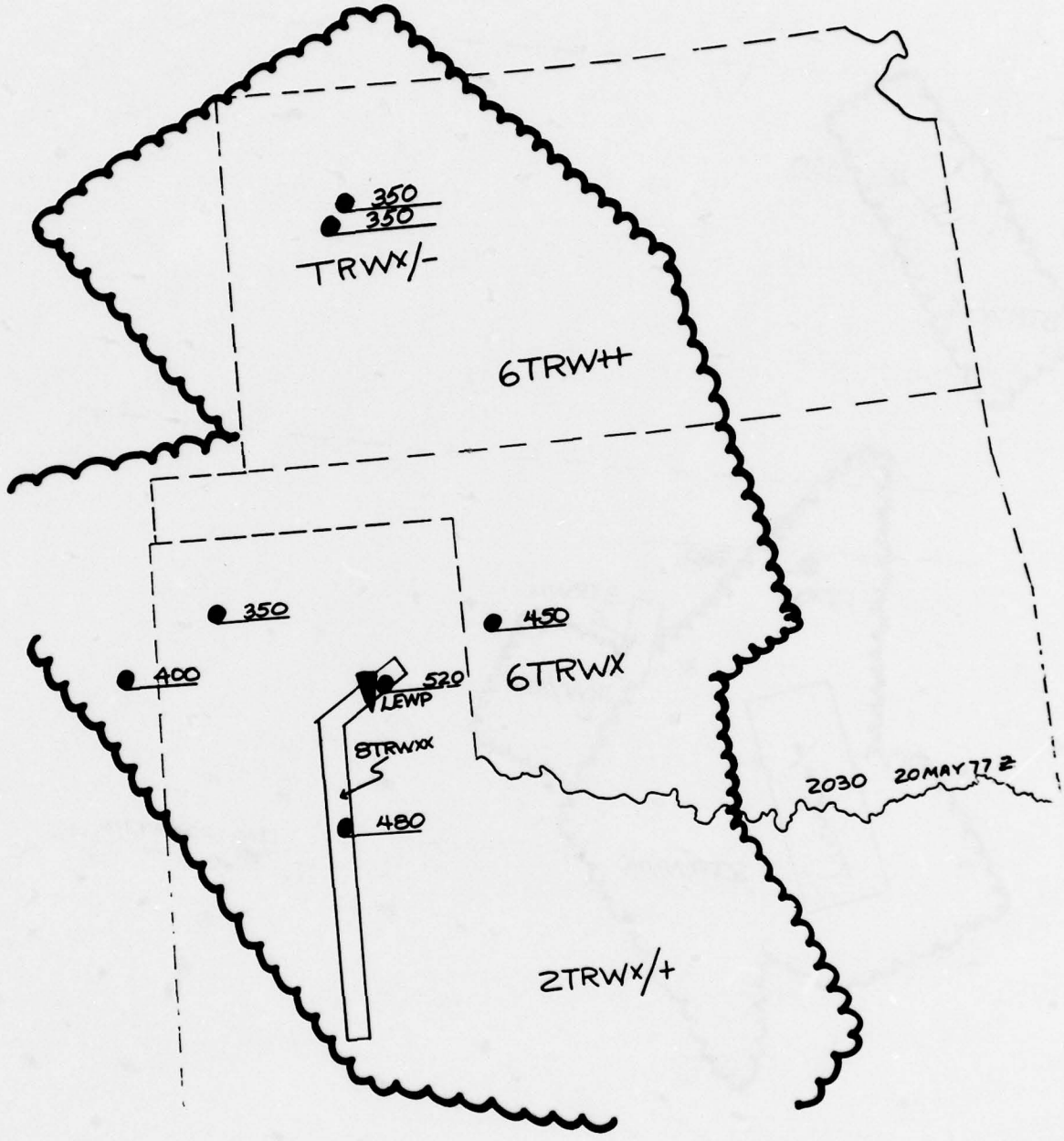

Figure A-6. Composite radar echoes for 2030Z, 20 May 77.

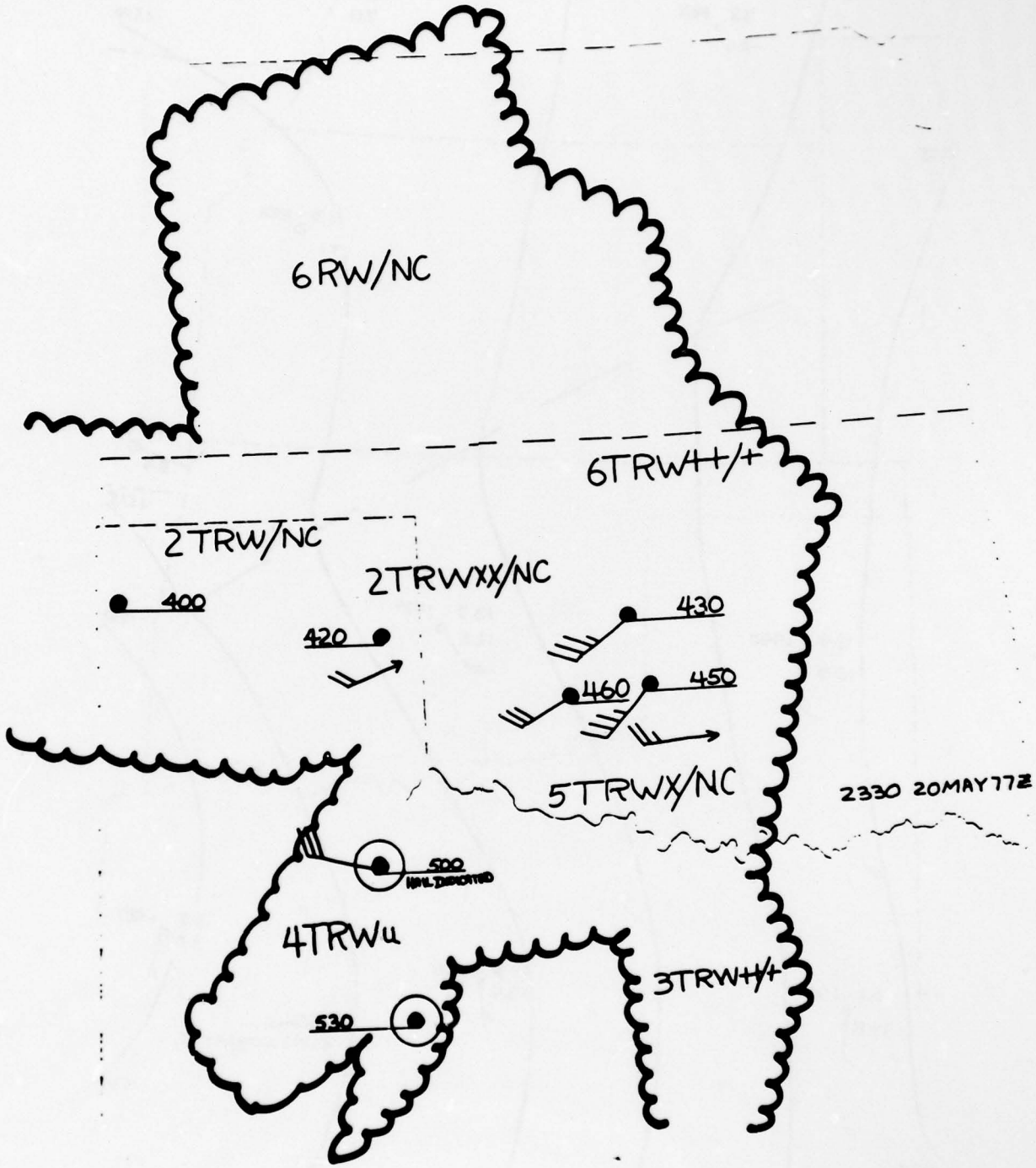

Figure A-7. Composite radar echoes for 2330Z, 20 May 77.

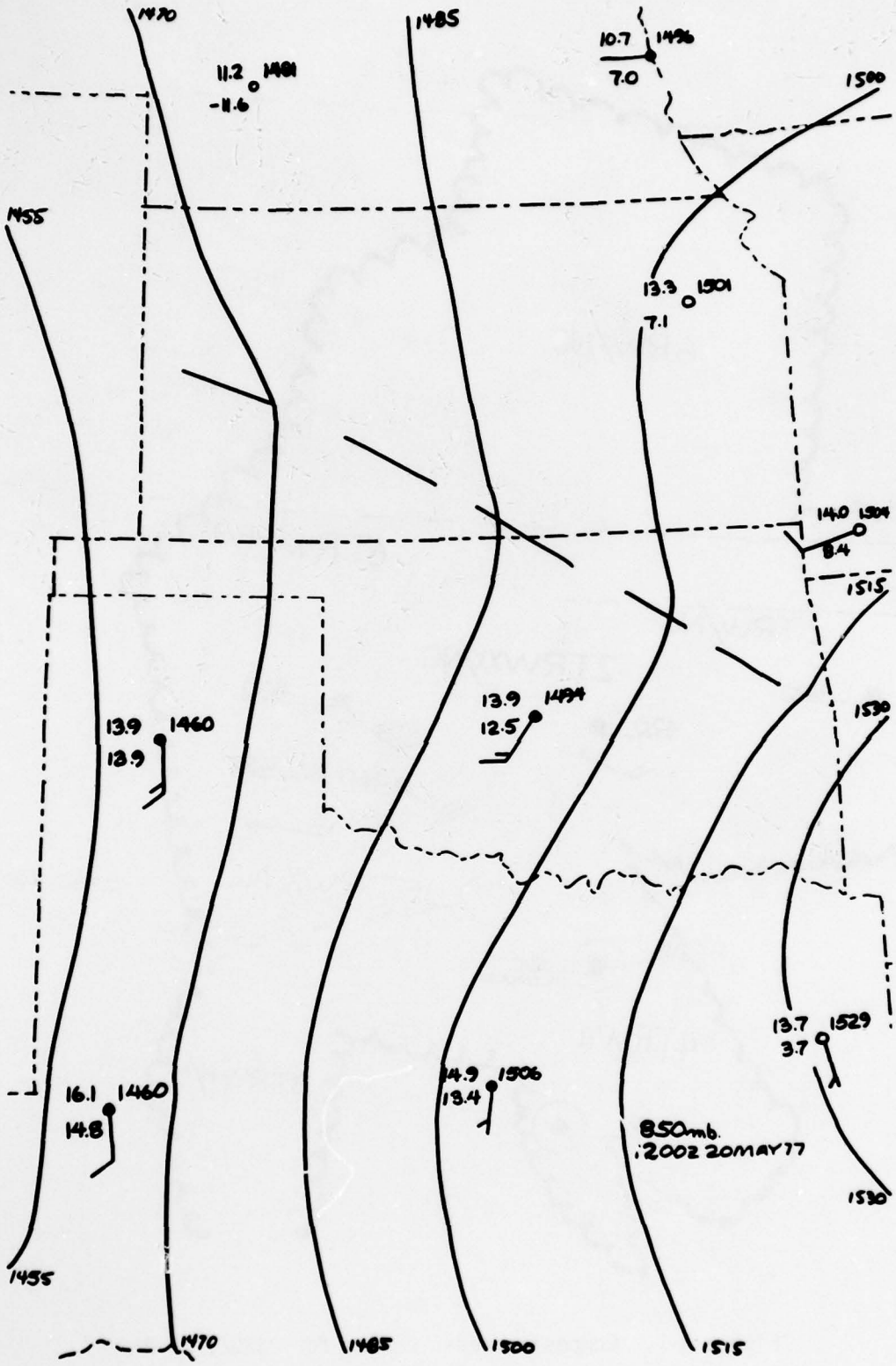

Figure A-8. Map for 850 mb, 1200Z, 20 May 77.

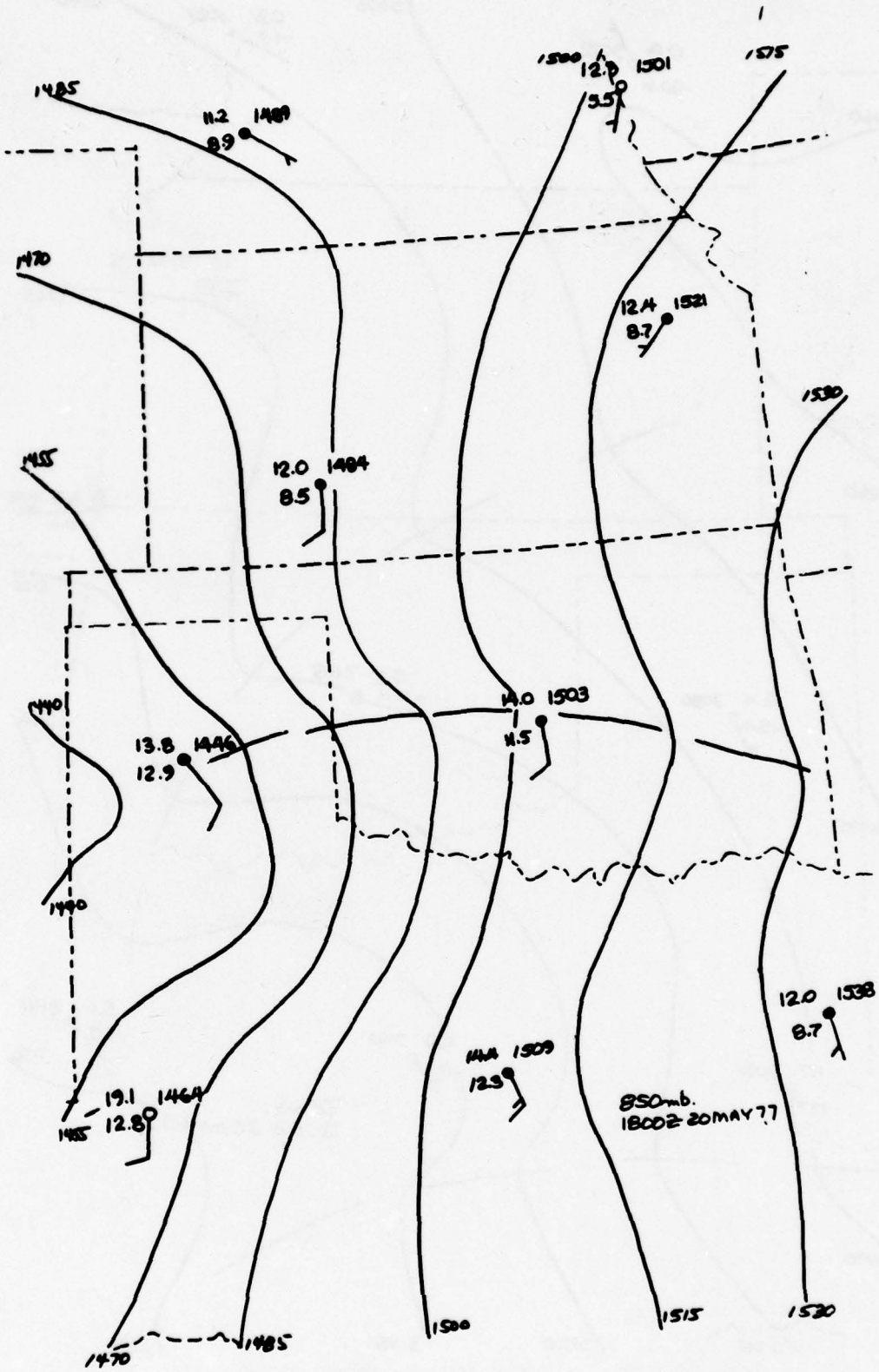

Figure A-9. Map for 850 mb, 1800Z, 20 May 77.

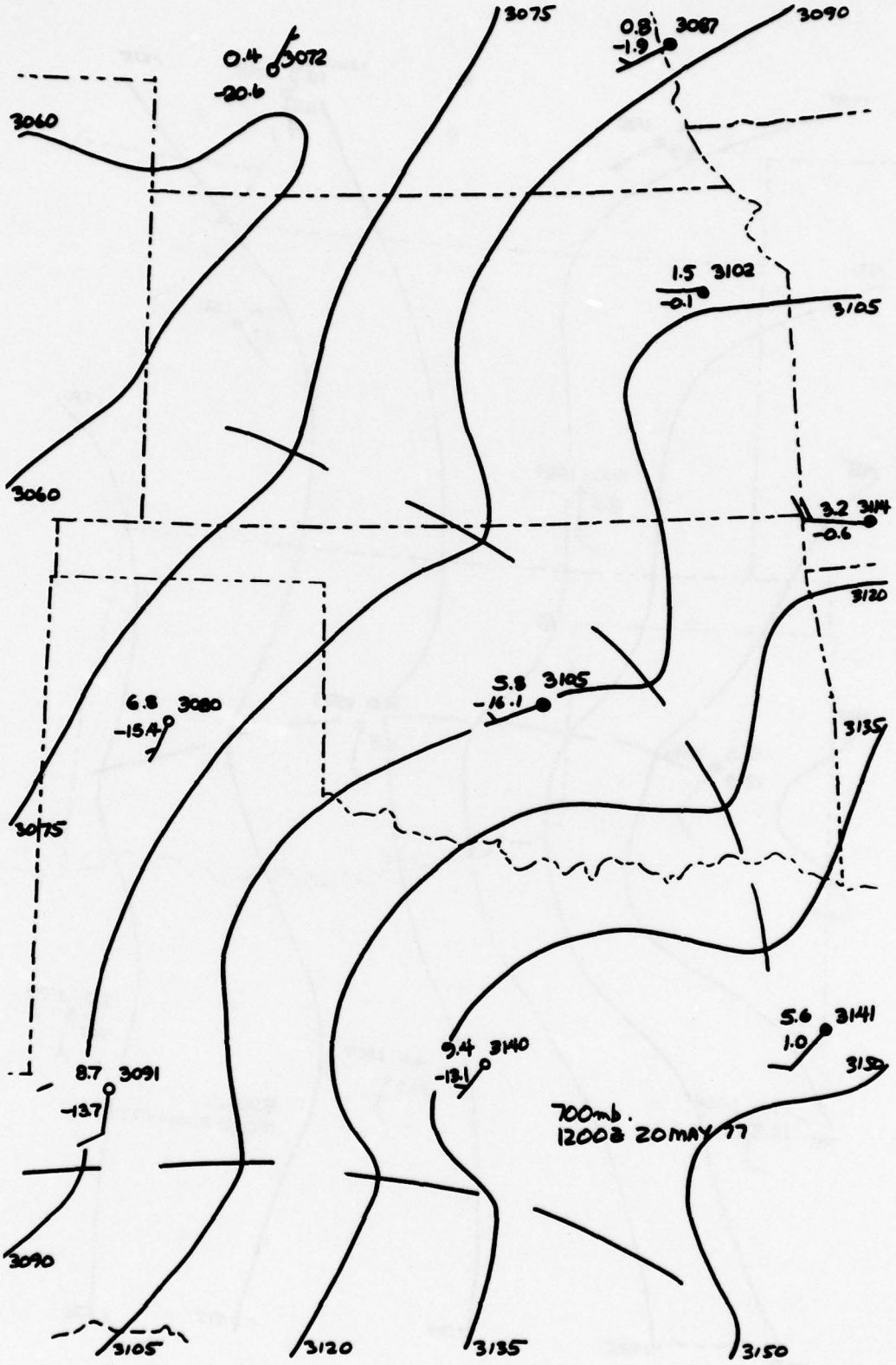

Figure A-10. Map for 700 mb, 1200Z, 20 May 77.

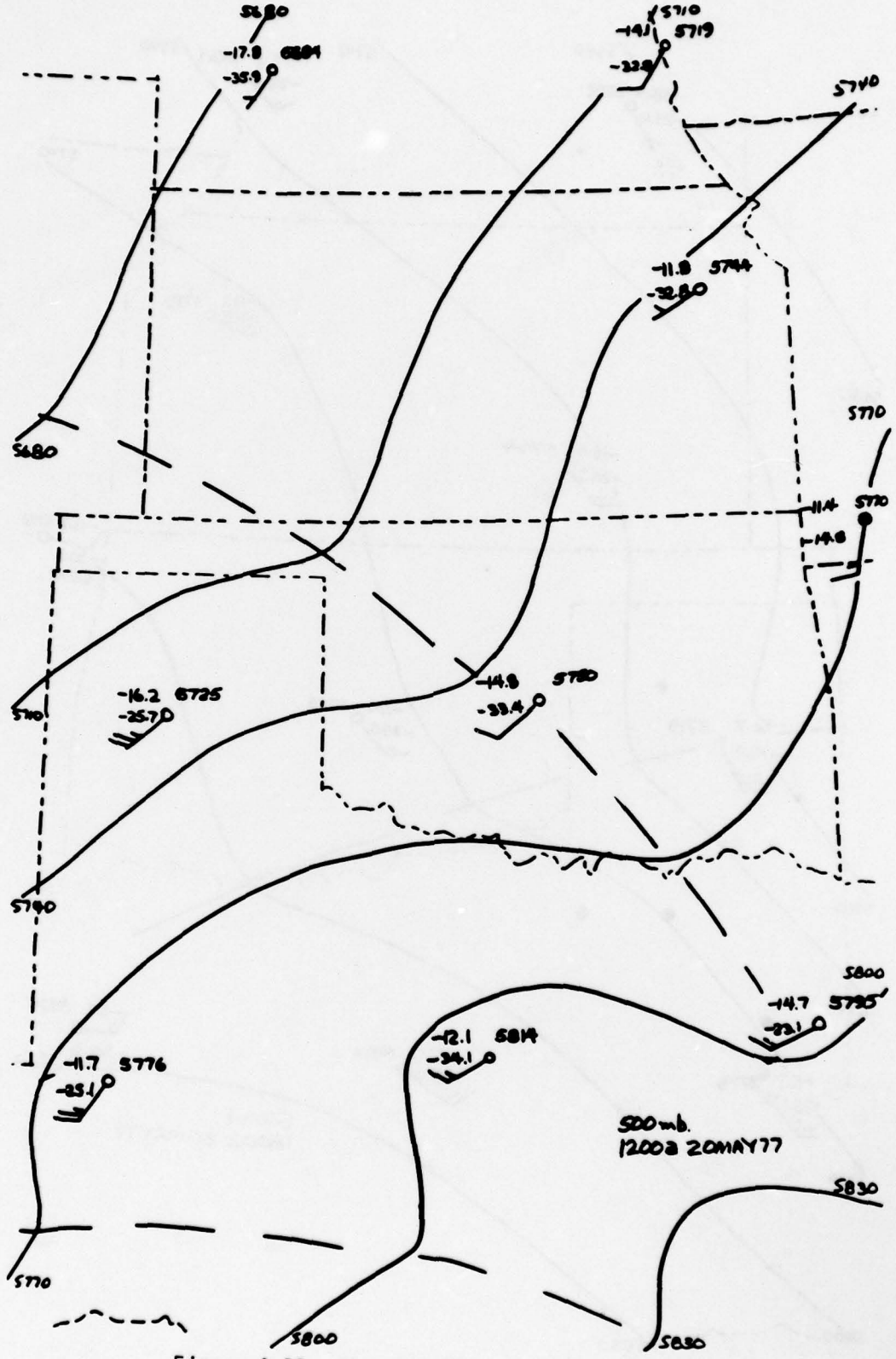

Figure A-11. Map for 500 mb, 1200Z, 20 May 77.

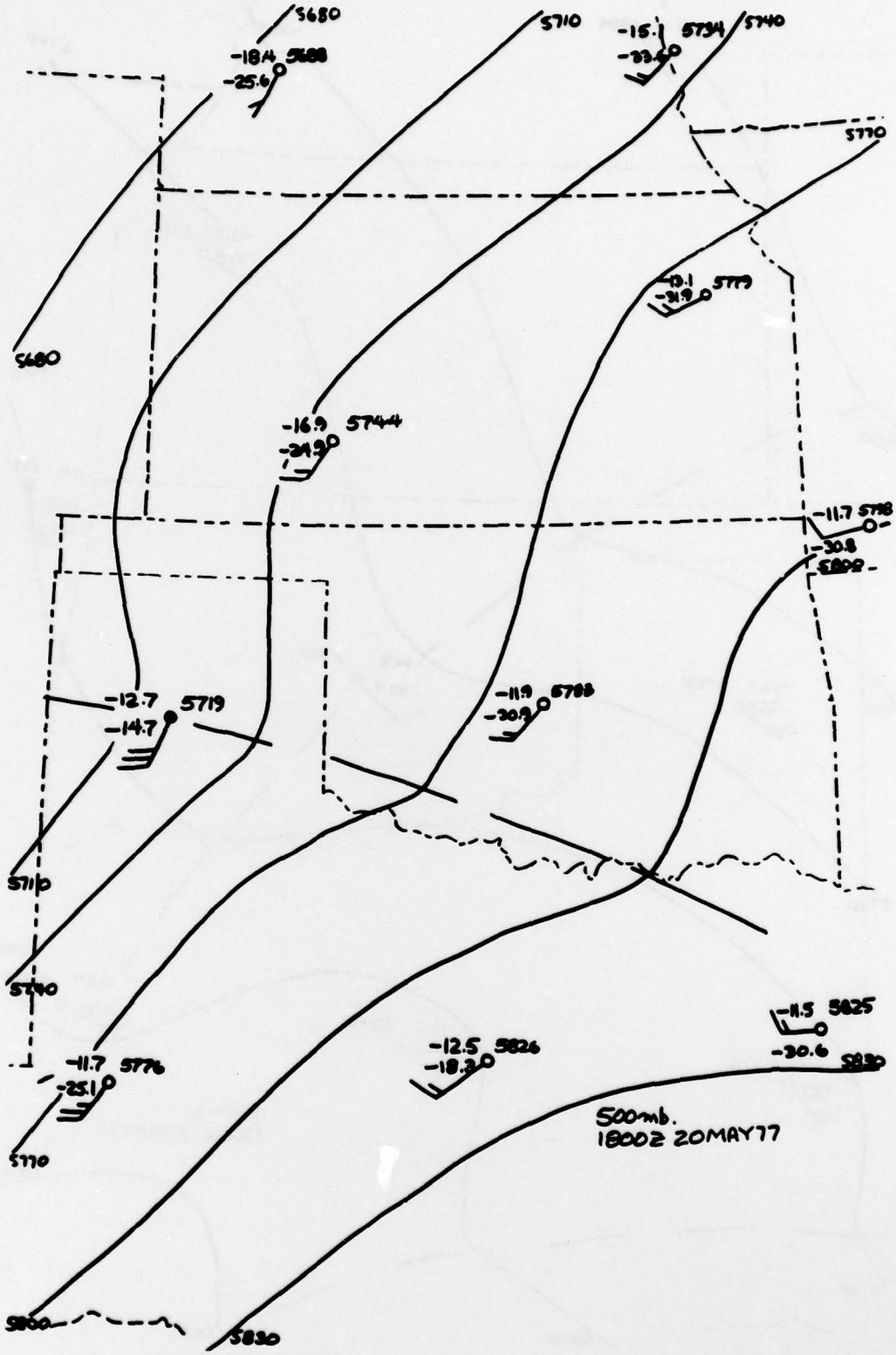

Figure A-12. Map for 500 mb, 1800Z, 20 May 77.

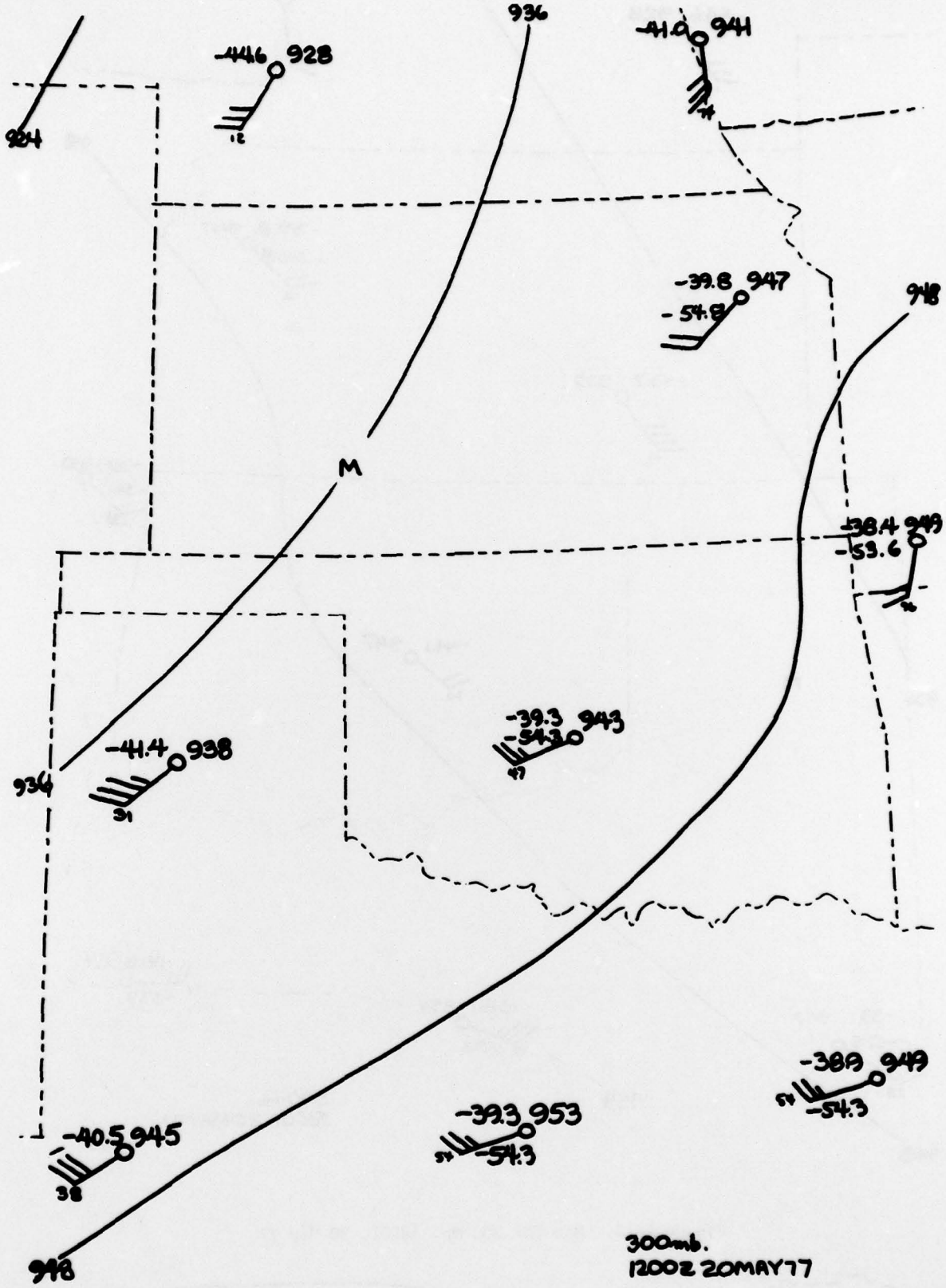

Figure A-13. Map for 300 mb, 1200Z, 20 May 77.

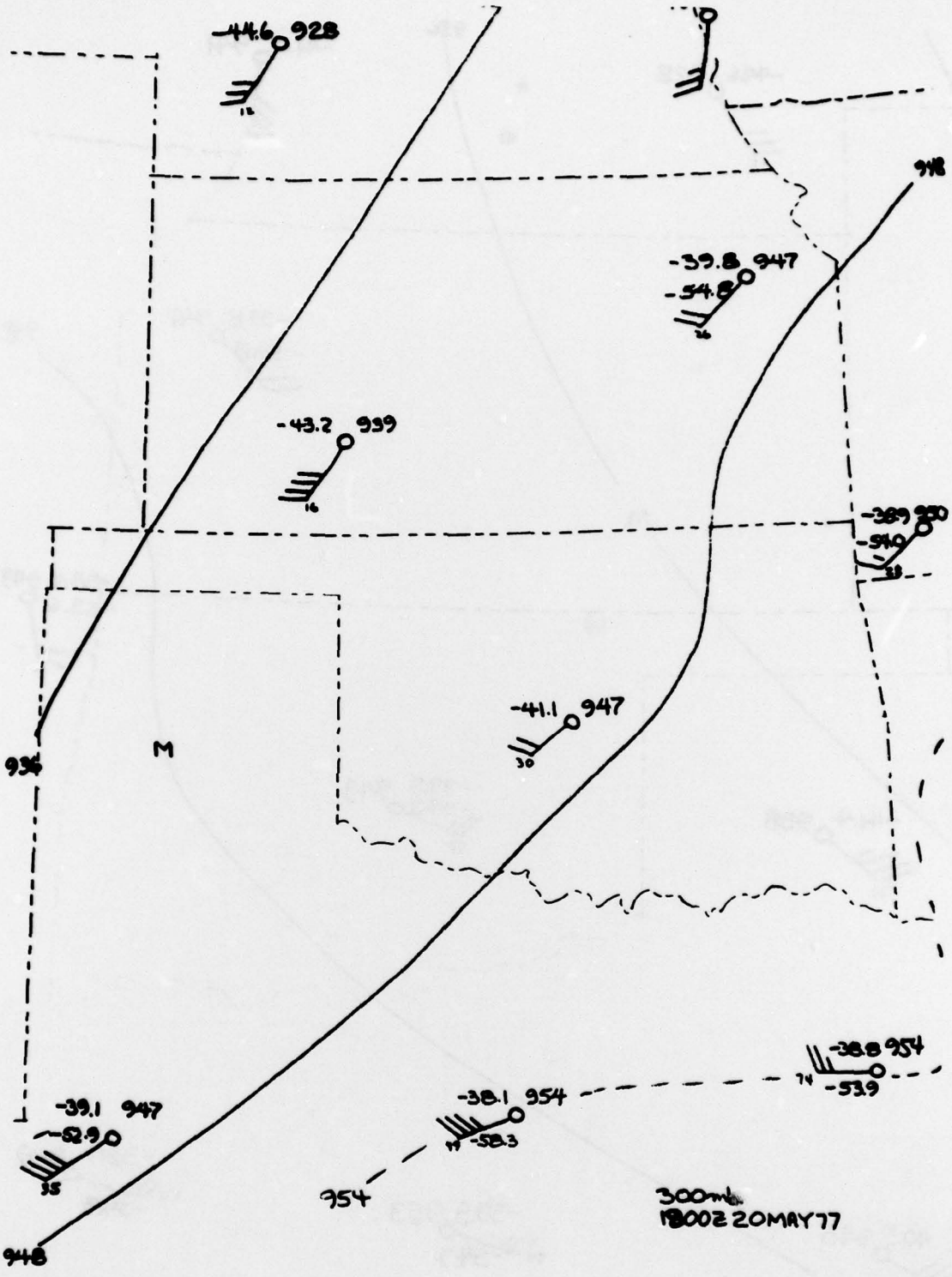

Figure A-14. Map for 300 mb, 1800Z, 20 May 77.

DISTRIBUTION LIST

Dr. Frank D. Eaton
Geophysical Institute
University of Alaska
Fairbanks, AK 99701

Commander
US Army Aviation Center
ATTN: ATZQ-D-MA
Fort Rucker, AL 36362

Chief, Atmospheric Sciences Div
Code ES-81
NASA
Marshall Space Flight Center,
AL 35812

Commander
US Army Missile R&D Command
ATTN: DRDMI-CGA (B. W. Fowler)
Redstone Arsenal, AL 35809

Redstone Scientific Information Center
ATTN: DRDMI-TBD
US Army Missile R&D Command
Redstone Arsenal, AL 35809

Commander
US Army Missile R&D Command
ATTN: DRDMI-TEM (R. Haraway)
Redstone Arsenal, AL 35809

Commander
US Army Missile R&D Command
ATTN: DRDMI-TRA (Dr. Essenwanger)
Redstone Arsenal, AL 35809

Commander
HQ, Fort Huachuca
ATTN: Tech Ref Div
Fort Huachuca, AZ 85613

Commander
US Army Intelligence Center & School
ATTN: ATSI-CD-MD
Fort Huachuca, AZ 85613

Commander
US Army Yuma Proving Ground
ATTN: Technical Library
Bldg 2100
Yuma, AZ 85364

Naval Weapons Center (Code 3173)
ATTN: Dr. A. Shlanta
China Lake, CA 93555

Sylvania Elec Sys Western Div
ATTN: Technical Reports Library
PO Box 205
Mountain View, CA 94040

Geophysics Officer
PMTC Code 3250
Pacific Missile Test Center
Point Mugu, CA 93042

Commander
Naval Ocean Systems Center (Code 4473)
ATTN: Technical Library
San Diego, CA 92152

Meteorologist in Charge
Kwajalein Missile Range
PO Box 67
APO San Francisco, CA 96555

Director
NOAA/ERL/APCL R31
RB3-Room 567
Boulder, CO 80302

Library-R-51-Tech Reports
NOAA/ERL
320 S. Broadway
Boulder, CO 80302

National Center for Atmos Research
NCAR Library
PO Box 3000
Boulder, CO 80307

R. B. Girardo
Bureau of Reclamation
E&R Center, Code 1220
Denver Federal Center, Bldg 67
Denver, CO 80225

National Weather Service
National Meteorological Center
W321, WWB, Room 201
ATTN: Mr. Quiroz
Washington, DC 20233

Mil Assistant for Atmos Sciences
Ofc of the Undersecretary of Defense
for Rsch & Engr/E&LS - Room 3D129
The Pentagon
Washington, DC 20301

Defense Communications Agency
Technical Library Center
Code 205
Washington, DC 20305

Director
Defense Nuclear Agency
ATTN: Technical Library
Washington, DC 20305

HQDA (DAEN-RDM/Dr. de Percin)
Washington, DC 20314

Director
Naval Research Laboratory
Code 5530
Washington, DC 20375

Commanding Officer
Naval Research Laboratory
Code 2627
Washington, DC 20375

Dr. J. M. MacCallum
Naval Research Laboratory
Code 1409
Washington, DC 20375

The Library of Congress
ATTN: Exchange & Gift Div
Washington, DC 20540
2

Head, Atmos Rsch Section
Div Atmospheric Science
National Science Foundation
1800 G. Street, NW
Washington, DC 20550

CPT Hugh Albers, Exec Sec
Interdept Committee on Atmos Science
National Science Foundation
Washington, DC 20550

Director, Systems R&D Service
Federal Aviation Administration
ATTN: ARD-54
2100 Second Street, SW
Washington, DC 20590

ADTC/DLODL
Eglin AFB, FL 32542

Naval Training Equipment Center
ATTN: Technical Library
Orlando, FL 32813

Det 11, 2WS/OI
ATTN: Maj Orondorff
Patrick AFB, FL 32925

USAFETAC/CB
Scott AFB, IL 62225

HQ, ESD/TOSI/S-22
Hanscom AFB, MA 01731

Air Force Geophysics Laboratory
ATTN: LCB (A. S. Carten, Jr.)
Hanscom AFB, MA 01731

Air Force Geophysics Laboratory
ATTN: LYD
Hanscom AFB, MA 01731

Meteorology Division
AFGL/LY
Hanscom AFB, MA 01731

US Army Liaison Office
MIT-Lincoln Lab, Library A-082
PO Box 73
Lexington, MA 02173

Director
US Army Ballistic Rsch Lab
ATTN: DRDAR-BLB (Dr. G. E. Keller)
Aberdeen Proving Ground, MD 21005

Commander
US Army Ballistic Rsch Lab
ATTN: DRDAR-BLP
Aberdeen Proving Ground, MD 21005

Director
US Army Armament R&D Command
Chemical Systems Laboratory
ATTN: DRDAR-CLJ-I
Aberdeen Proving Ground, MD 21010

Chief CB Detection & Alarms Div
Chemical Systems Laboratory
ATTN: DRDAR-CLC-CR (H. Tannenbaum)
Aberdeen Proving Ground, MD 21010

Commander
Harry Diamond Laboratories
ATTN: DELHD-CO
2800 Powder Mill Road
Adelphi, MD 20783

Commander
ERADCOM
ATTN: DRDEL-AP
2800 Powder Mill Road
Adelphi, MD 20783
2

Commander
ERADCOM
ATTN: DRDEL-CG/DRDEL-DC/DRDEL-CS
2800 Powder Mill Road
Adelphi, MD 20783

Commander
ERADCOM
ATTN: DRDEL-CT
2800 Powder Mill Road
Adelphi, MD 20783

Commander
ERADCOM
ATTN: DRDEL-EA
2800 Powder Mill Road
Adelphi, MD 20783

Commander
ERADCOM
ATTN: DRDEL-PA/DRDEL-ILS/DRDEL-E
2800 Powder Mill Road
Adelphi, MD 20783

Commander
ERADCOM
ATTN: DRDEL-PAO (S. Kimmel)
2800 Powder Mill Road
Adelphi, MD 20783

Chief
Intelligence Materiel Dev & Support Ofc
ATTN: DELEW-WL-I
Bldg 4554
Fort George G. Meade, MD 20755

Acquisitions Section, IRDB-D823
Library & Info Service Div, NOAA
6009 Executive Blvd
Rockville, MD 20852

Naval Surface Weapons Center
White Oak Library
Silver Spring, MD 20910

The Environmental Research
Institute of MI
ATTN: IRIA Library
PO Box 8618
Ann Arbor, MI 48107

Mr. William A. Main
USDA Forest Service
1407 S. Harrison Road
East Lansing, MI 48823

Dr. A. D. Belmont
Research Division
PO Box 1249
Control Data Corp
Minneapolis, MN 55440

Director
Naval Oceanography & Meteorology
NSTL Station
Bay St Louis, MS 39529

Director
US Army Engr Waterways Experiment Sta
ATTN: Library
PO Box 631
Vicksburg, MS 39180

Environmental Protection Agency
Meteorology Laboratory
Research Triangle Park, NC 27711

US Army Research Office
ATTN: DRXRO-PP
PO Box 12211
Research Triangle Park, NC 27709

Commanding Officer
US Army Armament R&D Command
ATTN: DRDAR-TSS Bldg 59
Dover, NJ 07801

Commander
HQ, US Army Avionics R&D Activity
ATTN: DAVAA-O
Fort Monmouth, NJ 07703

Commander/Director
US Army Combat Surveillance & Target
Acquisition Laboratory
ATTN: DELCS-D
Fort Monmouth, NJ 07703

Commander
US Army Electronics R&D Command
ATTN: DELCS-S
Fort Monmouth, NJ 07703

US Army Materiel Systems
Analysis Activity
ATTN: DRXSY-MP
Aberdeen Proving Ground, MD 21005

Director
US Army Electronics Technology &
Devices Laboratory
ATTN: DELET-D
Fort Monmouth, NJ 07703

Commander
US Army Electronic Warfare Laboratory
ATTN: DELEW-D
Fort Monmouth, NJ 07703

Commander
US Army Night Vision &
Electro-Optics Laboratory
ATTN: DELNV-L (Dr. Rudolf Buser)
Fort Monmouth, NJ 07703

Commander
ERADCOM Technical Support Activity
ATTN: DELSD-L
Fort Monmouth, NJ 07703

Project Manager, FIREFINDER
ATTN: DRCPM-FF
Fort Monmouth, NJ 07703

Project Manager, REMBASS
ATTN: DRCPM-RBS
Fort Monmouth, NJ 07703

Commander
US Army Satellite Comm Agency
ATTN: DRCPM-SC-3
Fort Monmouth, NJ 07703

Commander
ERADCOM Scientific Advisor
ATTN: DRDEL-SA
Fort Monmouth, NJ 07703

6585 TG/WE
Holloman AFB, NM 88330

AFWL/WE
Kirtland, AFB, NM 87117

AFWL/Technical Library (SUL)
Kirtland AFB, NM 87117

Commander
US Army Test & Evaluation Command
ATTN: STEWS-AD-L
White Sands Missile Range, NM 88002

Rome Air Development Center
ATTN: Documents Library
TSLD (Bette Smith)
Griffiss AFB, NY 13441

Commander
US Army Tropic Test Center
ATTN: STETC-TD (Info Center)
APO New York 09827

Commandant
US Army Field Artillery School
ATTN: ATSF-CD-R (Mr. Farmer)
Fort Sill, OK 73503

Commandant
US Army Field Artillery School
ATTN: ATSF-CF-R
Fort Sill, OK 73503

Director CFD
US Army Field Artillery School
ATTN: Met Division
Fort Sill, OK 73503

Commandant
US Army Field Artillery School
ATTN: Morris Swett Library
Fort Sill, OK 73503

Commander
US Army Dugway Proving Ground
ATTN: MT-DA-L
Dugway, UT 84022

Dr. C. R. Sreedrahan
Research Associates
Utah State University, UNC 48
Logan, UT 84322

Inge Dirmhirn, Professor
Utah State University, UNC 48
Logan, UT 84322

Defense Documentation Center
ATTN: DDC-TCA
Cameron Station Bldg 5
Alexandria, VA 22314
12

Commanding Officer
US Army Foreign Sci & Tech Center
ATTN: DRXST-IS1
220 7th Street, NE
Charlottesville, VA 22901

Naval Surface Weapons Center
Code G65
Dahlgren, VA 22448

Commander
US Army Night Vision
& Electro-Optics Lab
ATTN: DELNV-D
Fort Belvoir, VA 22060

Commander and Director
US Army Engineer Topographic Lab
ETL-TD-MB
Fort Belvoir, VA 22060

Director
Applied Technology Lab
DAVDL-EU-TSD
ATTN: Technical Library
Fort Eustis, VA 23604

Department of the Air Force
OL-C, 5WW
Fort Monroe, VA 23651

Department of the Air Force
5WW/DN
Langley AFB, VA 23665

Director
Development Center MCDEC
ATTN: Firepower Division
Quantico, VA 22134

US Army Nuclear & Chemical Agency
ATTN: MONA-WE
Springfield, VA 22150

Director
US Army Signals Warfare Laboratory
ATTN: DELSW-OS (Dr. R. Burkhardt)
Vint Hill Farms Station
Warrenton, VA 22186

Commander
US Army Cold Regions Test Center
ATTN: STECR-OP-PM
APO Seattle, WA 98733

Dr. John L. Walsh
Code 5560
Navy Research Lab
Washington, DC 20375

Commander
TRASANA
ATTN: ATAA-PL
(Dolores Anguiano)
White Sands Missile Range, NM 88002

Commander
US Army Dugway Proving Ground
ATTN: STEDP-MT-DA-M (Mr. Paul Carlson)
Dugway, UT 84022

Commander
US Army Dugway Proving Ground
ATTN: STEDP-MT-DA-T
(Mr. William Peterson)
Dugway, UT 84022

Commander
USATRADOC
ATTN: ATCD-SIE
Fort Monroe, VA 23651

Commander
USATRADOC
ATTN: ATCD-CF
Fort Monroe, VA 23651

Commander
USATRADOC
ATTN: Tech Library
Fort Monroe, VA 23651

ATMOSPHERIC SCIENCES RESEARCH PAPERS

1. Lindberg, J.D., "An Improvement to a Method for Measuring the Absorption Coefficient of Atmospheric Dust and other Strongly Absorbing Powders, " ECOM-5565, July 1975.
2. Avara, Elton, P., "Mesoscale Wind Shears Derived from Thermal Winds," ECOM-5566, July 1975.
3. Gomez, Richard B., and Joseph H. Pierluissi, "Incomplete Gamma Function Approximation for King's Strong-Line Transmittance Model," ECOM-5567, July 1975.
4. Blanco, A.J., and B.F. Engebos, "Ballistic Wind Weighting Functions for Tank Projectiles," ECOM-5568, August 1975.
5. Taylor, Fredrick J., Jack Smith, and Thomas H. Pries, "Crosswind Measurements through Pattern Recognition Techniques," ECOM-5569, July 1975.
6. Walters, D.L., "Crosswind Weighting Functions for Direct-Fire Projectiles," ECOM-5570, August 1975.
7. Duncan, Louis D., "An Improved Algorithm for the Iterated Minimal Information Solution for Remote Sounding of Temperature," ECOM-5571, August 1975.
8. Robbiani, Raymond L., "Tactical Field Demonstration of Mobile Weather Radar Set AN/TPS-41 at Fort Rucker, Alabama," ECOM-5572, August 1975.
9. Miers, B., G. Blackman, D. Langer, and N. Lorimier, "Analysis of SMS/GOES Film Data," ECOM-5573, September 1975.
10. Manquero, Carlos, Louis Duncan, and Rufus Bruce, "An Indication from Satellite Measurements of Atmospheric CO2 Variability," ECOM-5574, September 1975.
11. Petracca, Carmine, and James D. Lindberg, "Installation and Operation of an Atmospheric Particulate Collector," ECOM-5575, September 1975.
12. Avara, Elton P., and George Alexander, "Empirical Investigation of Three Iterative Methods for Inverting the Radiative Transfer Equation," ECOM-5576, October 1975.
13. Alexander, George D., "A Digital Data Acquisition Interface for the SMS Direct Readout Ground Station — Concept and Preliminary Design," ECOM-5577, October 1975.
14. Cantor, Israel, "Enhancement of Point Source Thermal Radiation Under Clouds in a Nonattenuating Medium," ECOM-5578, October 1975.
15. Norton, Colburn, and Glenn Hoidale, "The Diurnal Variation of Mixing Height by Month over White Sands Missile Range, N.M," ECOM-5579, November 1975.
16. Avara, Elton P., "On the Spectrum Analysis of Binary Data," ECOM-5580, November 1975.
17. Taylor, Fredrick J., Thomas H. Pries, and Chao-Huan Huang, "Optimal Wind Velocity Estimation," ECOM-5581, December 1975.
18. Avara, Elton P., "Some Effects of Autocorrelated and Cross-Correlated Noise on the Analysis of Variance, " ECOM-5582, December 1975.
19. Gillespie, Patti S., R.L. Armstrong, and Kenneth O. White, "The Spectral Characteristics and Atmospheric CO2 Absorption of the Ho^{+3}:YLF Laser at 2.05μm," ECOM-5583, December 1975.
20. Novlan, David J. "An Empirical Method of Forecasting Thunderstorms for the White Sands Missile Range," ECOM-5584, February 1976.
21. Avara, Elton P., "Randomization Effects in Hypothesis Testing with Autocorrelated Noise," ECOM-5585, February 1976.
22. Watkins, Wendell R., "Improvements in Long Path Absorption Cell Measurement," ECOM-5586, March 1976.
23. Thomas, Joe, George D. Alexander, and Marvin Dubbin, "SATTEL — An Army Dedicated Meteorological Telemetry System," ECOM-5587. March 1976.
24. Kennedy, Bruce W., and Delbert Bynum, "Army User Test Program for the RDT&E-XM-75 Meteorological Rocket," ECOM-5588, April 1976.

25. Barnett, Kenneth M., "A Description of the Artillery Meteorological Comparisons at White Sands Missle Range, October 1974 - December 1974 ('PASS' - Prototype Artillery [Meteorological] Subsystem)," ECOM-5589, April 1976.
26. Miller, Walter B., "Preliminary Analysis of Fall-of-Shot From Project 'PASS'," ECOM-5590, April 1976.
27. Avara, Elton P., "Error Analysis of Minimum Information and Smith's Direct Methods for Inverting the Radiative Transfer Equation," ECOM-5591, April 1976.
28. Yee, Young P., James D. Horn, and George Alexander, "Synoptic Thermal Wind Calculations from Radiosonde Observations Over the Southwestern United States," ECOM-5592, May 1976.
29. Duncan, Louis D., and Mary Ann Seagraves, "Applications of Empirical Corrections to NOAA-4 VTPR Observations," ECOM-5593, May 1976.
30. Miers, Bruce T., and Steve Weaver, "Applications of Meterological Satellite Data to Weather Sensitive Army Operations,"ECOM-5594, May 1976.
31. Sharenow, Moses, "Redesign and Improvement of Balloon ML-566," ECOM-5595, June, 1976.
32. Hansen, Frank V., "The Depth of the Surface Boundary Layer," ECOM-5596, June 1976.
33. Pinnick, R.G., and E.B. Stenmark, "Response Calculations for a Commercial Light-Scattering Aerosol Counter," ECOM-5597, July 1976.
34. Mason, J., and G.B. Hoidale, "Visibility as an Estimator of Infrared Transmittance," ECOM-5598, July 1976.
35. Bruce, Rufus E., Louis D. Duncan, and Joseph H. Pierluissi, "Experimental Study of the Relationship Between Radiosonde Temperatures and Radiometric-Area Temperatures," ECOM-5599, August 1976.
36. Duncan, Louis D., "Stratospheric Wind Shear Computed from Satellite Thermal Sounder Measurements," ECOM-5800, September 1976.
37. Taylor, F., P. Mohan, P. Joseph and T. Pries, "An All Digital Automated Wind Measurement System," ECOM-5801, September 1976.
38. Bruce, Charles, "Development of Spectrophones for CW and Pulsed Radiation Sources," ECOM-5802, September 1976.
39. Duncan, Louis D., and Mary Ann Seagraves,"Another Method for Estimating Clear Column Radiances," ECOM-5803, October 1976.
40. Blanco, Abel J., and Larry E. Taylor, "Artillery Meteorological Analysis of Project Pass," ECOM-5804, October 1976.
41. Miller, Walter, and Bernard Engebos," A Mathematical Structure for Refinement of Sound Ranging Estimates," ECOM-5805, November, 1976.
42. Gillespie, James B., and James D. Lindberg, "A Method to Obtain Diffuse Reflectance Measurements from 1.0 to 3.0 μm Using a Cary 17I Spectrophotometer," ECOM-5806, November 1976.
43. Rubio, Roberto, and Robert O. Olsen,"A Study of the Effects of Temperature Variations on Radio Wave Absorption,"ECOM-5807, November 1976.
44. Ballard, Harold N., "Temperature Measurements in the Stratosphere from Balloon-Borne Instrument Platforms, 1968-1975," ECOM-5808, December 1976.
45. Monahan, H.H., "An Approach to the Short-Range Prediction of Early Morning Radiation Fog," ECOM-5809, January 1977.
46. Engebos, Bernard Francis, "Introduction to Multiple State Multiple Action Decision Theory and Its Relation to Mixing Structures," ECOM-5810, January 1977.
47. Low, Richard D.H.,"Effects of Cloud Particles on Remote Sensing from Space in the 10-Micrometer Infrared Region," ECOM-5811, January 1977.
48. Bonner, Robert S., and R. Newton, "Application of the AN/GVS-5 Laser Rangefinder to Cloud Base Height Measurements," ECOM-5812, February 1977.
49. Rubio, Roberto, "Lidar Detection of Subvisible Reentry Vehicle Erosive Atmospheric Material," ECOM-5813, March 1977.
50. Low, Richard D.H., and J.D. Horn, "Mesoscale Determination of Cloud-Top Height: Problems and Solutions," ECOM-5814, March 1977.

51. Duncan, Louis D., and Mary Ann Seagraves, "Evaluation of the NOAA-4 VTPR Thermal Winds for Nuclear Fallout Predictions," ECOM-5815, March 1977.
52. Randhawa, Jagir S., M. Izquierdo, Carlos McDonald and Zvi Salpeter, "Stratospheric Ozone Density as Measured by a Chemiluminescent Sensor During the Stratcom VI-A Flight," ECOM-5816, April 1977.
53. Rubio, Roberto, and Mike Izquierdo, "Measurements of Net Atmospheric Irradiance in the 0.7- to 2.8-Micrometer Infrared Region," ECOM-5817, May 1977.
54. Ballard, Harold N., Jose M. Serna, and Frank P. Hudson Consultant for Chemical Kinetics, "Calculation of Selected Atmospheric Composition Parameters for the Mid-Latitude, September Stratosphere," ECOM-5818, May 1977.
55. Mitchell, J.D., R.S. Sagar, and R.O. Olsen, "Positive Ions in the Middle Atmosphere During Sunrise Conditions," ECOM-5819, May 1977.
56. White, Kenneth O., Wendell R. Watkins, Stuart A. Schleusener, and Ronald L. Johnson, "Solid-State Laser Wavelength Identification Using a Reference Absorber," ECOM-5820, June 1977.
57. Watkins, Wendell R., and Richard G. Dixon, "Automation of Long-Path Absorption Cell Measurements," ECOM-5821, June 1977.
58. Taylor, S.E., J.M. Davis, and J.B. Mason, "Analysis of Observed Soil Skin Moisture Effects on Reflectance," ECOM-5822, June 1977.
59. Duncan, Louis D. and Mary Ann Seagraves, "Fallout Predictions Computed from Satellite Derived Winds," ECOM-5823. June 1977.
60. Snider, D.E., D.G. Murcray, F.H. Murcray, and W.J. Williams, "Investigation of High-Altitude Enhanced Infrared Backround Emissions" (U), SECRET, ECOM-5824, June 1977.
61. Dubbin, Marvin H. and Dennis Hall, "Synchronous Meteorlogical Satellite Direct Readout Ground System Digital Video Electronics," ECOM-5825, June 1977.
62. Miller, W., and B. Engebos, "A Preliminary Analysis of Two Sound Ranging Algorithms," ECOM-5826, July 1977.
63. Kennedy, Bruce W., and James K. Luers, "Ballistic Sphere Techniques for Measuring Atomspheric Parameters," ECOM-5827, July 1977.
64. Duncan, Louis D., "Zenith Angle Variation of Satellite Thermal Sounder Measurements," ECOM-5828, August 1977.
65. Hansen, Frank V., "The Critical Richardson Number," ECOM-5829, September 1977.
66. Ballard, Harold N., and Frank P. Hudson (Compilers), "Stratospheric Composition Balloon-Borne Experiment," ECOM-5830, October 1977.
67. Barr, William C., and Arnold C. Peterson, "Wind Measuring Accuracy Test of Meteorological Systems," ECOM-5831, November 1977.
68. Ethridge, G.A. and F.V. Hansen, "Atmospheric Diffusion: Similarity Theory and Empirical Derivations for Use in Boundary Layer Diffusion Problems," ECOM-5832, November 1977.
69. Low, Richard D.H., "The Internal Cloud Radiation Field and a Technique for Determining Cloud Blackness," ECOM-5833, December 1977.
70. Watkins, Wendell R., Kenneth O. White, Charles W. Bruce, Donald L. Walters, and James D. Lindberg, "Measurements Required for Prediction of High Energy Laser Transmission," ECOM-5834, December 1977.
71. Rubio, Robert, "Investigation of Abrupt Decreases in Atmospherically Backscattered Laser Energy," ECOM-5835. December 1977.
72. Monahan, H.H. and R.M. Cionco, "An Interpretative Review of Existing Capabilities for Measuring and Forecasting Selected Weather Variables (Emphasizing Remote Means)," ASL-TR-0001, January 1978.
73. Heaps, Melvin G., "The 1979 Solar Eclipse and Validation of D-Region Models," ASL-TR-0002. March 1978.

74. Jennings, S.G., and J.B. Gillespie, "M.I.E. Theory Sensitivity Studies - The Effects of Aerosol Complex Refractive Index and Size Distribution Variations on Extinction and Absorption Coefficients Part II: Analysis of the Computational Results," ASL-TR-0003, March 1978.
75. White, Kenneth O. et al, "Water Vapor Continuum Absorption in the 3.5μm to 4.0μm Region," ASL-TR-0004, March 1978.
76. Olsen, Robert O., and Bruce W. Kennedy, "ABRES Pretest Atmospheric Measurements," ASL-TR-0005, April 1978.
77. Ballard, Harold N., Jose M. Serna, and Frank P. Hudson, "Calculation of Atmospheric Composition in the High Latitude September Stratosphere," ASL-TR-0006, May 1978.
78. Watkins, Wendell R. et al, "Water Vapor Absorption Coefficients at HF Laser Wavelengths," ASL-TR-0007, May 1978.
79. Hansen, Frank V., "The Growth and Prediction of Nocturnal Inversions," ASL-TR-0008, May 1978.
80. Samuel, Christine, Charles Bruce, and Ralph Brewer, "Spectrophone Analysis of Gas Samples Obtained at Field Site," ASL-TR-0009, June 1978.
81. Pinnick, R.G. et al., "Vertical Structure in Atmospheric Fog and Haze and its Effects on IR Extinction," ASL-TR-0010, July 1978.
82. Low, Richard D.H., Louis D. Duncan, and Richard B. Gomez, "The Microphysical Basis of Fog Optical Characterization," ASL-TR-0011, August 1978.
83. Heaps, Melvin G., "The Effect of a Solar Proton Event on the Minor Neutral Constituents of the Summer Polar Mesosphere," ASL-TR-0012, August 1978.
84. Mason, James B., "Light Attenuation in Falling Snow," ASL-TR-0013, August 1978.
85. Blanco, Abel J., "Long-Range Artillery Sound Ranging: "PASS" Meteorological Application," ASL-TR-0014, September 1978.
86. Heaps, M.G., and F.E. Niles, "Modeling the Ion Chemistry of the D-Region: A case Study Based Upon the 1966 Total Solar Eclipse," ASL-TR-0015, September 1978.
87. Jennings, S.G., and R.G. Pinnick, "Effects of Particulate Complex Refractive Index and Particle Size Distribution Variations on Atmospheric Extinction and Absorption for Visible Through Middle-Infrared Wavelengths," ASL-TR-0016, September 1978.
88. Watkins, Wendell R., Kenneth O. White, Lanny R. Bower, and Brian Z. Sojka, " Pressure Dependence of the Water Vapor Continuum Absorption in the 3.5- to 4.0-Micrometer Region," ASL-TR-0017, September 1978.
89. Miller, W.B., and B.F. Engebos, "Behavior of Four Sound Ranging Techniques in an Idealized Physical Enviroment," ASL-TR-0018, September 1978.
90. Gomez, Richard G., "Effectiveness Studies of the CBU-88/B Bomb, Cluster, Smoke Weapon" (U), CONFIDENTIAL ASL-TR-0019, September 1978.
91. Miller, August, Richard C. Shirkey, and Mary Ann Seagraves, "Calculation of Thermal Emission from Aerosols Using the Doubling Technique," ASL-TR-0020, November, 1978.
92. Lindberg, James D. et al., "Measured Effects of Battlefield Dust and Smoke on Visible, Infrared, and Millimeter Wavelengths Propagation: A Preliminary Report on Dusty Infrared Test-I (DIRT-I)," ASL-TR-0021, January 1979.
93. Kennedy, Bruce W., Arthur Kinghorn, and B.R. Hixon, "Engineering Flight Tests of Range Meteorological Sounding System Radiosonde," ASL-TR-0022, February 1979.
94. Rubio, Roberto, and Don Hoock, "Microwave Effective Earth Radius Factor Variability at Wiesbaden and Balboa," ASL-TR-0023, February 1979.
95. Low, Richard D.H., "A Theoretical Investigation of Cloud/Fog Optical Properties and Their Spectral Correlations," ASL-TR-0024, February 1979.

96. Pinnick, R.G., and H.J. Auvermann, "Response Characteristics of Knollenberg Light-Scattering Aerosol Counters," ASL-TR-0025, February 1979.
97. Heaps, Melvin G., Robert O. Olsen, and Warren W. Berning, "Solar Eclipse 1979, Atmospheric Sciences Laboratory Program Overview," ASL-TR-0026 February 1979.
98. Blanco, Abel J., "Long-Range Artillery Sound Ranging: 'PASS' GR-8 Sound Ranging Data," ASL-TR-0027, March 1979.
99. Kennedy, Bruce W., and Jose M. Serna, "Meteorological Rocket Network System Reliability," ASL-TR-0028, March 1979.
100. Swingle, Donald M., "Effects of Arrival Time Errors in Weighted Range Equation Solutions for Linear Base Sound Ranging," ASL-TR-0029, April 1979.
101. Umstead, Robert K., Ricardo Pena, and Frank V. Hansen, "KWIK: An Algorithm for Calculating Munition Expenditures for Smoke Screening/Obscuration in Tactical Situations," ASL-TR-0030, April 1979.
102. D'Arcy, Edward M., "Accuracy Validation of the Modified Nike Hercules Radar," ASL-TR-0031, May 1979.
103. Rodriguez, Ruben, "Evaluation of the Passive Remote Crosswind Sensor," ASL-TR-0032, May 1979.
104. Barber, T.L., and R. Rodriguez, "Transit Time Lidar Measurement of Near-Surface Winds in the Atmosphere," ASL-TR-0033, May 1979.
105. Low, Richard D.H., Louis D. Duncan, and Y.Y. Roger R. Hsiao, "Microphysical and Optical Properties of California Coastal Fogs at Fort Ord," ASL-TR-0034, June 1979.
106. Rodriguez, Ruben, and William J. Vechione, "Evaluation of the Saturation Resistant Crosswind Sensor," ASL-TR-0035, July 1979
107. Ohmstede, William D., "The Dynamics of Material Layers," ASL-TR-0036, July 1979.
108. Pinnick, R.G., S.G. Jennings, Petr Chýlek, and H.J. Auvermann "Relationships between IR Extinction, Absorption, and Liquid Water Content of Fogs," ASL-TR-0037, August 1979
109. Rodriguez, Ruben, and William J. Vechione, "Performance Evaluation of the Optical Crosswind Profiler," ASL-TR-0038, August 1979
110. Miers, Bruce T., "Precipitation Estimation Using Satellite Data" ASL-TR-0039, September 1979

☆ U.S.GOVERNMENT PRINTING OFFICE: 1979 — 677-017/32